Duality

1974 Rep. Prog. Phys. 37 1035

(http://iopscience.iop.org/0034-4885/37/8/002)

Duality

R J N PHILLIPS AND D P ROY

Rutherford High Energy Laboratory, Chilton, Didcot, Berkshire

Abstract

In elementary particle physics, low energy interactions are characterized by resonance formation and high energy interactions by Regge pole exchanges: two quite different and apparently unrelated mechanisms. Duality is the hypothesis that they are in fact simply and quantitatively related. The present review describes the background and motivation for this hypothesis, and the different degrees of severity with which it can be formulated, together with some of its most notable predictions. Applications to the scattering amplitude are discussed in § 3; the most significant results being exchange degeneracy for high energy scattering and the Regge interpolation of resonances at low energy. Section 4 describes applications to particle classification. Duality constraints tie together several SU(3) multiplets, like a higher symmetry scheme; the exoticity prediction for the baryon–antibaryon channel is discussed in detail. Section 5 describes duality diagrams that provide a simple prescription for deriving most of the duality results. Section 6 is about the Veneziano model, a simple form of amplitude that satisfies duality explicitly; extensions to multiparticle scattering are also sketched. The final section discusses applications of duality to the inclusive reaction, which is a field of immense activity at present. The most significant results are again exchange degeneracy and the Regge interpolation of resonances—this time for the regions of high and low missing mass.

This review was completed in July 1973.

Rep. Prog. Phys. 1974 **37** 1035–1097

Contents

1. Introduction

In elementary particle physics, duality is the name of a simple and direct relation postulated to hold between low energy and high energy scattering mechanisms. It began as a guess, based on a little experience, but is now recognized as a rather general class of theoretical hypothesis. To appreciate its significance, one must first realize that there is no unified calculable theory of all elementary particle phenomena yet; there are workable theories all right, but they apply to limited ranges of effects, and relations between them exist in principle rather than in practice. Thus the dynamical mechanisms used to describe and systematize high energy scattering were not, in practical terms, closely related to the mechanisms of low energy scattering. Duality connects these apparently disconnected regimes.

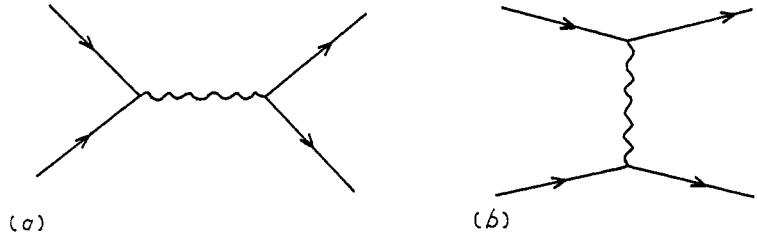

Figure 1. (*a*) Resonance formation; (*b*) particle exchange.

For low energy interactions, the dominant dynamical features are resonances, which are unstable particle states that are formed and subsequently decay in various channels as illustrated by the Feynman diagram 1(*a*). They give a fluctuating energy dependence. Typically, resonances give bumps in total cross sections at the resonant energies. The resonant partial wave amplitudes are changing rapidly here, so differential cross sections and polarizations also fluctuate rapidly. As energy increases, however, the resonances become more closely spaced and also wider, and their overlapping smooths out the fluctuations.

At high energies, the dominant mechanism is supposed to be Regge pole exchange, indicated in figure 1(*b*). This is essentially Yukawa's old idea of virtual particle exchange, but in the modern version the exchanged particle not only has a virtual energy–momentum vector but also a virtual spin. The resulting energy dependence is smooth.

Both the resonance and Regge pole mechanisms depend on intermediate single-particle states, which are the simple and basic things in S matrix theory. This is an attractive feature. However when it comes to details the two mechanisms are totally dissimilar and apparently disconnected. Each regime has been extensively studied by itself and many systematic features are known. The beauty of duality is that it relates these two sets of systematics. At an empirical level, duality is very successful in correlating many apparently unrelated phenomena and in predicting new relationships. At a deeper level, duality puts powerful constraints on the underlying theory, with profound dynamical consequences.

An example may suggest some of the power and the surprise of duality predictions. Suppose two particles $a+b$ have no resonances in their low energy interaction. Then, for their high energy interaction, duality predicts that the amplitudes are purely real for all non-diffractive scatterings $a+b\to c+d$, and that the total $a+b$ cross section is approximately independent of energy.

So much for the commercials. We hope this introduction gives some idea of what duality means, to non-specialist readers, because this is probably where we part company. To get any further, we must confront some technicalities. It is necessary to know a few things about the resonance and Regge pole mechanisms, before a connection between them can be properly understood and appreciated. For semi-specialist readers, like a new graduate student in high energy physics, §2 summarizes what is needed about analyticity, crossing symmetry and Regge poles. Section 3 gives more precise definitions: duality can in fact be sharpened and stated with various degrees of severity. Subsequent sections describe the classification of particle multiplets, duality diagrams and dual models. The final section is devoted to duality in the inclusive reaction. The inclusive reaction is currently a field of intense activity, and duality plays a very significant role here.

This is a good place to mention other reviews of duality. We especially recommend the Schladming lectures of Jacob (1969) and Kugler (1970), and the Brookhaven lectures of Harari (1969b). For a more thorough introduction to S matrix theory and Regge poles, see standard textbooks such as Omnès and Froissart (1963), Jacob and Chew (1964), Barger and Cline (1968); see also reviews such as Phillips and Ringland (1972).

2. Preliminaries

2.1. Analyticity and crossing

Figure 2 shows a general two-body scattering. In fact, it represents any of the three processes

$$\begin{aligned} &a+b\to c+d \quad (s \text{ channel})\\ &a+\bar{c}\to \bar{b}+d \quad (t \text{ channel})\\ &a+\bar{d}\to c+\bar{b} \quad (u \text{ channel}) \end{aligned} \tag{2.1}$$

or these time-reversed. The usual kinematic invariants are

$$\begin{aligned} s &= (p_a+p_b)^2\\ t &= (p_a-p_c)^2\\ u &= (p_a-p_d)^2 \end{aligned} \tag{2.2}$$

which obey the constraint $s+t+u = m_a^2+m_b^2+m_c^2+m_d^2$, where particle i has mass m_i and 4-momentum p_i. These variables have different physical meanings in different channels. In the s channel, s is the square of total centre of mass energy, while the other two are invariant squares of momentum transfer (their roles are permuted in the t and u channels).

Crossing symmetry says that not only a single picture, but also a single invariant scattering amplitude $A(s, t, u)$, describes all three channels above. Since the physical regions for different channels do not overlap, the connection between them is made by analytic continuation. Typically, we may fix $t<0$ and define $\nu = s-u$ as the remaining independent variable. Then $A(\nu)$ is analytic in the ν plane, with cuts

along the real axis from ν_s to ∞ and from ν_u to $-\infty$, where ν_x corresponds to the lowest x channel threshold. There may also be isolated poles on the real axis, corresponding to bound states in one or other channel. Figure 3 shows where the s channel and u channel physical regions are and how to continue between them.

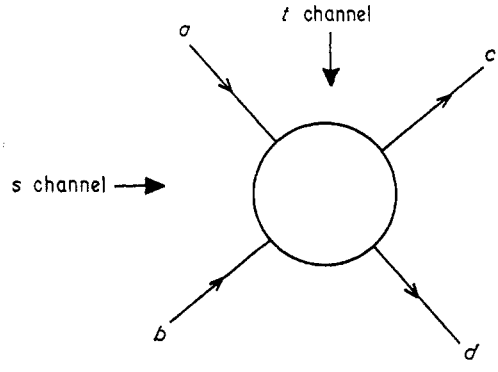

Figure 2. General two-body scattering process.

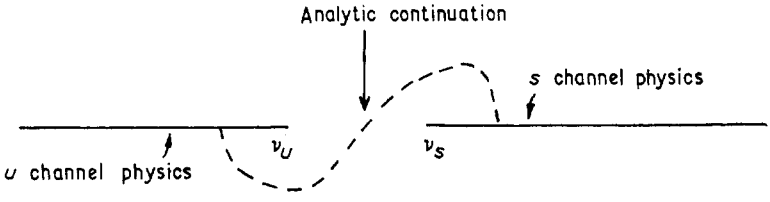

Figure 3. The s and u channel physical regions in the complex ν plane.

Analytic continuation also relates the formation of a t channel resonance (in the physical region $t >$ threshold, u and s generally < 0) with the exchange of a t channel particle in high energy forward s channel scattering (where $s > 0$, $t < 0$, $u \simeq -s$). A continuation in both s and t is needed; fortunately Regge poles offer a simple way to do it as shown below.

2.2. Regge poles

A stable particle in the t channel implies a pole in the scattering amplitude $A(s, t, u)$ at $t = m^2$. For a resonance, the pole lies off the real axis. To describe low energy t channel scattering near the resonance, we can use a Breit–Wigner form like

$$A = \frac{\mathrm{P}_J(\cos\theta_t)}{t - m^2 + im\Gamma} + \text{background} \tag{2.3}$$

where m, Γ, J are the resonance mass, width and spin. This is for particle formation.

However there are difficulties in adapting equation (2.3) for particle exchange. If we simply continue the pole term to $t < 0$ using

$$\cos\theta_t = \frac{2s + t - 4M^2}{t - 4M^2}$$

where equal external masses M are assumed for convenience, we find $A \simeq s^J$ and hence $\mathrm{d}\sigma/\mathrm{d}t \simeq s^{2J-2}$ in high energy s channel scattering. For $J > 1$ this conflicts both with experiment and with theoretical bounds.

Regge poles offer an alternative that approximates to equation (2.3) for particle formation but continues to something more acceptable for particle exchange. A t channel Regge pole is characterized by a trajectory function $\alpha(t)$, a residue function $\beta(t)$ and a signature $\tau = \pm 1$; it gives an amplitude

$$A(\text{Regge}) = \beta \frac{P_\alpha(-\cos\theta_t) + \tau P_\alpha(\cos\theta_t)}{\sin\pi\alpha} \tag{2.4}$$

where P_α is a Legendre function of degree α. As we vary t, $\alpha(t)$ varies. When α goes through a physical (integer) value J, the vanishing denominator in equation (2.4) gives a pole. Half these poles are killed by the symmetry of the numerator; for even (odd) signature, only poles with even (odd) spin J survive. Thus the Regge pole generates a sequence of particles, with increasing masses and spins, as illustrated in figure 4 for the ρ trajectory. Both $\alpha(t)$ and $\beta(t)$ are real for $t <$ threshold, but have imaginary parts for $t >$ threshold, so resonance poles are off the real t axis as required. Near each particle, A(Regge) reduces to the Breit–Wigner form.

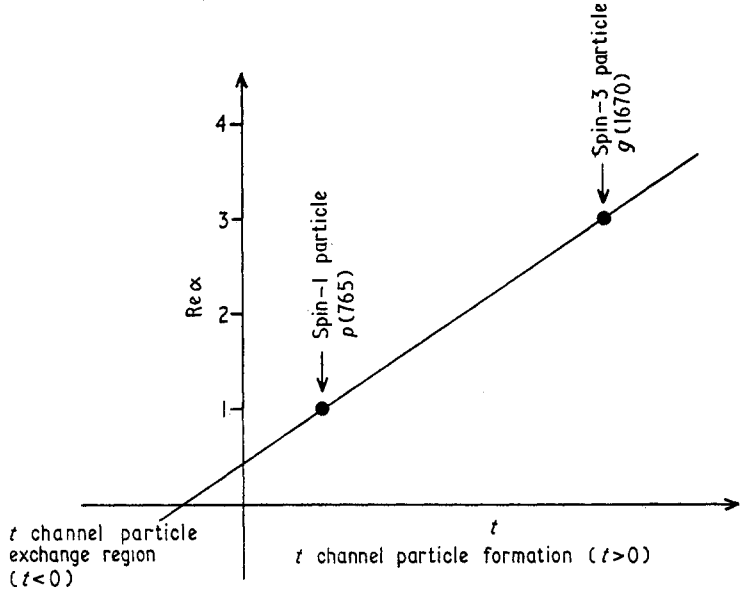

Figure 4. Plot of Re $\alpha(t)$ against t for the odd-signature ρ Regge pole.

The signature factor $P_\alpha(-\cos\theta_t) + \tau P_\alpha(\cos\theta_t)$ in equation (2.4) ensures that the Regge pole term has a pure symmetry under the interchange $\cos\theta_t \leftrightarrow -\cos\theta_t$, as needed in physical applications. For example, $\pi\pi$ scattering with isospin $I = 1$ has an antisymmetric amplitude, and odd-signature Regge poles are appropriate.

For high energy scattering in the s or u channel, which is the particle exchange regime, equation (2.4) reduces to

$$A^s(\text{Regge}) = \gamma \frac{1 + \tau e^{-i\pi\alpha}}{\sin\pi\alpha} \left(\frac{s}{s_0}\right)^\alpha \quad \text{for } s \to \infty \tag{2.5a}$$

$$A^u(\text{Regge}) = \tau\gamma \frac{1 + \tau e^{-i\pi\alpha}}{\sin\pi\alpha} \left(\frac{u}{s_0}\right)^\alpha \quad \text{for } u \to \infty \tag{2.5b}$$

where $\gamma(t)$ is a product of $\beta(t)$ and other factors, and s_0 is an arbitrary energy scale.

Note that A^s and A^u have the same phase, coming from the signature factor $1+\tau\exp(-i\pi\alpha)$ and γ is real. The corresponding contributions to cross sections behave like

$$\sigma_T{}^s \simeq \frac{\operatorname{Im} A_{el}{}^s(t=0)}{s} \simeq s^{\alpha(0)-1} \tag{2.6}$$

$$d\sigma^s/dt \simeq \frac{|A^s|^2}{s^2} \simeq s^{2\alpha(t)-2} \tag{2.7}$$

and similarly in the u channel. This is acceptable provided $\alpha(t) \leqslant 1$ for $t \leqslant 0$.

The relative importance of Regge poles in high energy scattering depends on their trajectories α. Elastic scattering is supposed to be dominated by the Pomeranchuk pole P ('pomeron'), with $\tau_P = 1$ and $\alpha_P(0) = 1$; this gives constant asymptotic cross sections, obeying the Pomeranchuk theorem, $\sigma^s(\infty) = \sigma^u(\infty)$. The pomeron seems rather special; no particles are yet associated with it in the region $t > 0$ and it may be just a convenient parametrization of diffractive effects.

There are also Regge poles associated with all the known particles. They appear to have trajectory intercepts $\alpha(0) \leqslant 0{\cdot}5$ and slopes $d\alpha/dt$ of order 1 GeV^{-2}. They control non-diffractive inelastic processes, and give subasymptotic corrections to elastic scattering.

The t channel Regge pole picture is generally used only for small t (up to a few GeV^2), ie forward scattering in the s channel. Similarly u channel Regge poles are invoked for backward scattering in the s channel.

2.2.1. Factorization. This is an important property: $\gamma(t)$ factors into two parts, one for each vertex. For a t channel $a\bar{c} \to \bar{b}d$ we have

$$\gamma(t) = \tilde{\gamma}_{a\bar{c}}(t)\,\tilde{\gamma}_{\bar{b}d}(t). \tag{2.8}$$

This is a familiar property of resonance formation, carried over to particle exchange. It interrelates channels, strongly constraining the Regge contributions.

Spin. The above account strictly applies to spinless particle scattering. When the external particles a, b, c, d have spin, some of the details change. There are now generally several independent amplitudes, referring to different s channel helicity states for example; equations (2.5)–(2.8) hold for each separate amplitude. Note that all contributions from one Regge pole have the same phase. For factorization, we must be a little more careful; helicities must now be specified at each vertex and different kinematic factors in γ arise with different helicities. But if these kinematic factors are appropriately separated, the s channel helicity amplitudes still factorize, to leading order in s.

Baryon exchanges (half-integral J) bring some further complications: see below.

2.2.2. Exchange degeneracy. A Regge pole refers only to odd-J or even-J states in the t channel, because of its signature. However, in special situations Regge poles may occur in degenerate pairs, with opposite signatures but with the same trajectory and residue functions; $\alpha^+ = \alpha^-$, $\gamma^+ = \gamma^-$ (or alternatively $\gamma^+ = -\gamma^-$). This is called 'exchange degeneracy', abbreviated to EXD. We shall see that duality constraints often imply such EXD relations.

Striking consequences follow, if a single EXD-pair of t channel Regge poles dominates high energy s channel (and u channel) scattering. If their residues γ are

equal in the s channel, then their residues γ in the u channel have opposite signs; adding them together and using equation (2.5) with $\tau = +1$ and -1 we get

$$A^s = \frac{2\gamma}{\sin \pi\alpha} \left(\frac{s}{s_0}\right)^\alpha \tag{2.9a}$$

$$A^u = \frac{2\gamma}{\sin \pi\alpha} e^{-i\pi\alpha} \left(\frac{u}{s_0}\right)^\alpha \tag{2.9b}$$

Thus the amplitudes are equal in modulus, the phase is real in the s channel, and rotates with $\alpha(t)$ in the u channel. Hence the cross sections are equal, within spin-weight factors

$$(2S_a+1)\frac{d\sigma^s}{dt} = (2S_c+1)\frac{d\sigma^u}{dt} \tag{2.10}$$

where S_a, S_c are the spins of a, c. Furthermore, since all the helicity amplitudes in the s channel have the same real phase (and all the u channel amplitudes have the same rotating phase), and since vector polarization effects $\mathscr{P}$ depend on interference terms like $\mathrm{Im}\, f_1 f_2^*$ between different helicity amplitudes f_i, it follows that all such polarizations vanish, ie

$$\mathscr{P}^s = 0 \tag{2.11a}$$

$$\mathscr{P}^u = 0. \tag{2.11b}$$

The s and u channels are sometimes said to be related by 'line-reversal', and equations (2.9)–(2.11) are called 'line-reversal relations'.

If more than one EXD-pair of poles are important, most of these results are lost, with only the reality of A^s and the vanishing of $\mathscr{P}^s$ remaining.

2.2.3. Wrong-signature zeros. In the Regge pole amplitudes given by equation (2.5), the factors $[1+\tau\exp(-i\pi\alpha)]/\sin\pi\alpha$ give a pole when $\alpha(t)$ goes through a 'right-signature' integer—ie even (odd) when τ is $+1$ (-1). For $t<0$ such poles are unphysical, corresponding to particles with $(\text{mass})^2<0$ and giving infinite s and u channel scattering, therefore they must be suppressed by dynamical zeros of $\gamma(t)$. Various mechanisms for zeros of γ have been proposed.

Do such mechanisms also act at wrong-signature integers? If so, since there are no poles to kill, they will give zeros of the amplitudes (wrong-signature zeros, or WSZ). There are plausible arguments for WSZ, perhaps the best is based on EXD. If a pair of Regge poles are EXD in some channel, a single function $\gamma(t)$ must kill the right-signature poles for both $\tau = +1$ and $\tau = -1$—ie have zeros at *all* integers. These zeros propagate to other channels via factorization.

Some authors call WSZ simply 'signature zeros' which is a good name. If γ kills all the poles of $1/\sin\pi\alpha$, we are left just with the zeros of the signature factor $1+\tau\exp(-i\pi\alpha)$.

2.2.4. Baryon exchange. We generally talk about baryons in the u channel, because in typical meson–baryon scattering $\mathrm{MB}\to\mathrm{MB}$ the u channel $\overline{\mathrm{M}}\mathrm{B}\to\overline{\mathrm{M}}\mathrm{B}$ has baryon quantum numbers while the t channel $\mathrm{M}\overline{\mathrm{M}}\to\mathrm{B}\overline{\mathrm{B}}$ does not.

Baryons bring some special features.

(i) Because particle spins are half-integral, we replace the signature factor in equation (2.5) by $[1+i\exp(-i\pi\alpha)]/\cos\pi\alpha$.

(ii) Baryon Regge poles occur in pairs, describing particles with the same signature but opposite parity. In the conventional treatment the two trajectories α

are independent for $u>0$ but coincide at $u=0$ and are complex conjugates for $u<0$; residues γ are similarly related.

(iii) Since α and γ are generally complex for $u<0$, the phase of a Regge term is no longer given just by the signature factor.

Exchange degeneracy is more complicated now. However, if pairs of u channel Regge poles with opposite signatures have common α and γ, the net s channel amplitudes are still real. Furthermore if α is real the corresponding amplitudes for t channel scattering are equal apart from a phase factor $\mathrm{i}\exp(-\mathrm{i}\pi\alpha)$.

2.2.5. Regge cuts. A t channel Regge pole is really a pole of the partial wave amplitude $A_J(t)$ that moves in the J plane as t varies. There can also be branch-points of A_J with associated cuts. Mandelstam showed that cuts can come from diagrams where two Regge poles are exchanged, like Figure 5. A cut contributes like a continuum of Regge poles:

$$A(\text{cut}) = \int_{-\infty}^{\alpha_c} \mathrm{d}\alpha'\, \rho(\alpha')\, A(\text{Regge};\, \alpha') \tag{2.12}$$

where α_c is the branch point and ρ is a weight function.

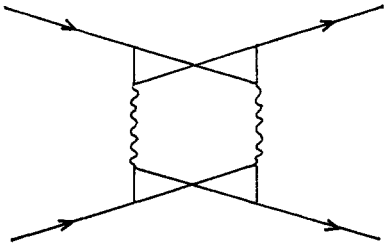

Figure 5. Double Regge pole exchange that gives a Regge cut.

Physically, cuts therefore represent double-particle (or multi-particle) exchanges, or (where the pomeron is concerned) a rescattering correction. Unfortunately there is yet no reliable way to calculate cut contributions, only some *ad hoc* models. However, we know some general properties, such as

(i) asymptotic behaviour and crossing, like a Regge pole term with $\alpha=\alpha_c$, apart from logarithms of s (or u);

(ii) for two Regge poles $\alpha_i=\alpha_{i0}+\alpha_i' t$, the branch point is

$$\alpha_{12} = \alpha_{10}+\alpha_{20}-1+\frac{t\alpha_1'\alpha_2'}{\alpha_1'+\alpha_2'};$$

(iii) signature $\tau_{12}=\tau_1\tau_2$ (except for two-baryon exchange when $\tau_{12}=-\tau_1\tau_2$).

If we distinguish the pomeron P from other Regge poles R, these properties imply that P+P cuts behave like contributions to P, P+R cuts are like corrections ('absorptive corrections') to R, and R+R cuts are in a class of their own (genuine 2-particle exchanges).

2.3. Finite energy sum rules

Finite energy sum rules (FESR) are a useful consequence of analyticity and Regge behaviour. If we take an amplitude $A(s,t,u)$ at fixed t, defining $\nu=(s-u)/2M$ as the free variable (with M the target mass), $A(\nu)$ is real analytic in the cut ν plane of figure 3. Cauchy's theorem now says that $\int_C A(\nu)\,\mathrm{d}\nu=0$, integrating round any closed contour C that does not enclose any singularities.

Suppose we take the contour C in figure 6. Physics is on the real axis, so the upper and lower semicircles of C are apparently unphysical. But if we assume the Regge behaviour of equation (2.5) for the high energy physical region with $|\nu| \geqslant N$, writing ν^α in place of $(s/s_0)^\alpha$, we can continue this prescription analytically into the complex ν plane and use it to evaluate the unphysical contours in terms of physical (Regge) parameters. Thus Cauchy's theorem relates integrals of low energy physical amplitudes (along the real axis with $|\nu| \leqslant N$) to high energy Regge parameters.

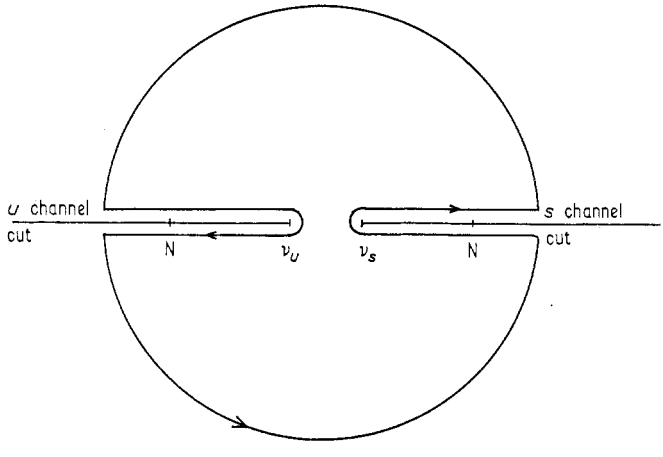

Figure 6. The integration contour C.

We can do the same with any moment $\nu^n A(\nu)$ instead of just $A(\nu)$. The discontinuity across the cut is $2i\nu^n \operatorname{Im} A$, and so the resulting FESR is

$$\int_{-N}^{\nu_u} + \int_{\nu_s}^{N} d\nu\, \nu^n \operatorname{Im} A(\nu) = 2 \sum_i \gamma_i \frac{N^{\alpha_i+n+1}}{\alpha_i+n+1}. \tag{2.13}$$

Here the sum is over Regge poles i with $\tau_i = +1$ (-1) only when n = odd (even); contributions of the opposite signature vanish, through the symmetry of the integral.

This FESR looks even simpler if the integrand $\nu^n A$ is precisely antisymmetric in ν. For example if $A(\nu) = -A(\nu)$ and n is even, the left and righthand cut integrals are equal, and we get

$$\int_{\nu_s}^{N} \operatorname{Im} A(\nu)\, \nu^n\, d\nu = \sum_i \gamma_i \frac{N^{\alpha_i+n+1}}{\alpha_i+n+1}. \tag{2.14}$$

This is the simplest prototype FESR, found in textbooks. Many refinements are possible, such as introducing more sophisticated weight functions than ν^n, but the idea of relating low energy integrals to high energy Regge parameters remains the same. It is a starting point for duality.

2.4. Exotic channels

Resonances are found to occur in some channels and not in others. Empirically, the channels where they are found are exactly those of the quark model that describes mesons and baryons as quark–antiquark ($q\bar{q}$) and three-quark (qqq) states,

respectively. Channels are said to be 'exotic' if they do not fall into the $q\bar{q}$ or qqq categories. The absence of observed resonances in exotic channels is an important systematic of low energy scattering and an important constraint on theory.

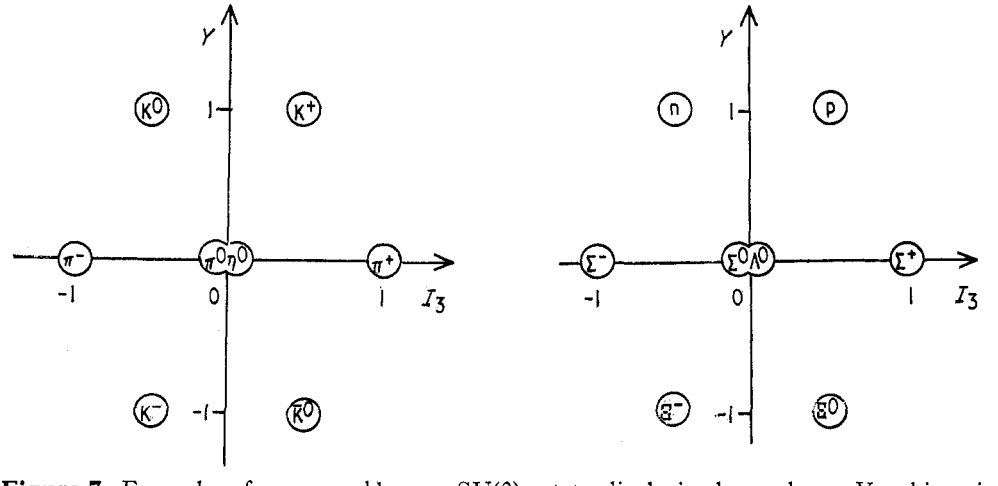

Figure 7. Examples of meson and baryon SU(3) octets, displaying hypercharge Y and isospin component I_3 (charge $Q = I_3 + \frac{1}{2}Y$).

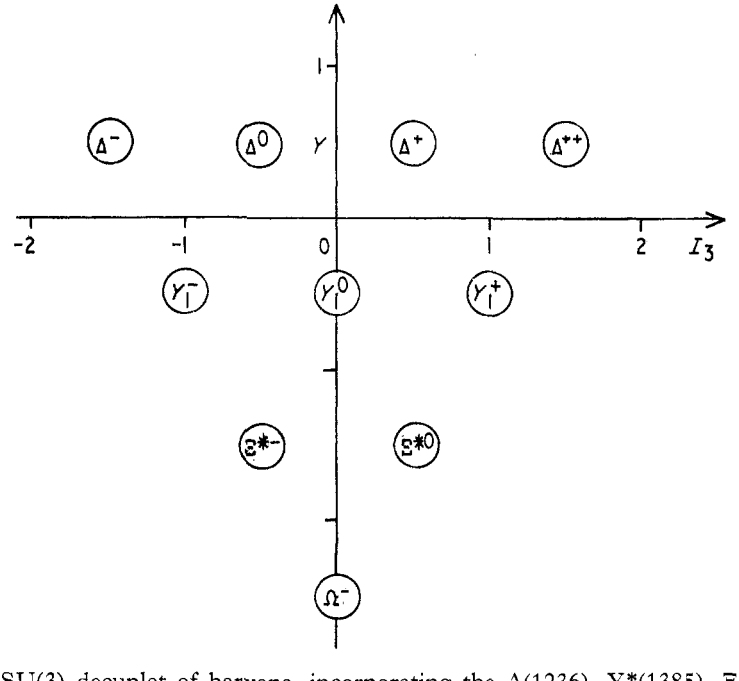

Figure 8. SU(3) decuplet of baryons, incorporating the $\Delta(1236)$, $Y_1^*(1385)$, $\Xi^*(1530)$ and $\Omega(1672)$ isospin multiplets.

The SU(3) representations of allowed meson resonances are thus [1] and [8], while [1], [8] and [10] are allowed for baryons. Examples of meson and baryon octets and decuplets are shown in figures 7 and 8, exhibiting the isospin and hypercharge quantum numbers. The isospin-zero member of an octet has the same

isospin quantum numbers as an SU(3) singlet, so with SU(3)-breaking these two states become mixed. This happens for instance with the η and η' pseudoscalar mesons.

The quark model forbids certain assignments of G parity because of the charge conjugation properties of the $q\bar{q}$ system. For spin J and isospin I, it forbids natural parity states with $P = (-)^J$ and $G = (-)^{J+I+1}$, and the unnatural parity state with $J = 0$, $P = -1$ and $G = +1$. No resonances with such quantum numbers have been found. They are called 'exotics of the second kind', to distinguish them from SU(3)-exotics.

For an introduction to the quark model, see Dalitz (1966).

3. Phenomenological versions of duality

We have seen that the high energy s channel scattering is described well by the leading Regge exchanges in the t channel. One can, of course, define a Regge background consisting of lower lying Regge singularities and a genuine background integral (the latter representing the fact that an expansion of the scattering amplitude in terms of Regge singularities converges only asymptotically), and thereby one can build up a formal Regge description of the scattering amplitude at any given energy. Alternatively one can formally define a non-resonant background and add to the s channel resonance contributions to describe the scattering amplitude at any given energy.

One would thus have established a complete equivalence between the s channel resonance and t channel Regge pictures. Such a formal equivalence would, however, be hardly useful since the background is only a euphemism for our domain of ignorance in the resonance or the Regge picture. Any meaningful connection between the two pictures has to rely on a possible overlap between the leading Regge exchanges in the t channel and the resonance part of the s channel description.

It has been recognized for a number of years now that the leading Regge exchange provides a good description of the scattering amplitude over a wide energy range down to a few GeV. A particularly simple example is the charge exchange pion nucleon scattering. The t channel quantum numbers suggest that the leading Regge exchange here is simply the ρ pole, and possibly the ρ–P (pomeron) cut, which has the same quantum numbers and a similar effective trajectory as the ρ pole. Phenomenological analyses of the charge exchange π–N scattering data have shown that the leading Regge exchange is adequate down to a laboratory momentum of 3 GeV, ie to a centre of mass system energy of about 2·5 GeV.

In the context of the s channel resonance picture, however, the role of the background has been the subject of a long controversy. Until a few years ago, it was universally believed that the background must constitute the bulk of the scattering amplitude from a few hundred MeV upwards in the laboratory momentum. This was partly due to the apparent smoothness of the scattering amplitude in this range (eg the solid line in figure 10), and partly this was a hangover from our understanding (or rather the lack of it) of the resonance spectrum in the early sixties, when a few low-lying resonances (essentially the ones shown in figures 7 and 8) were believed to exhaust the entire spectrum. Obviously the background must describe the scattering amplitude in a range where there are no resonances. However, our understanding of the resonance physics has changed radically since then. Rich arrays of resonances have been discovered in the entire sub-Regge region

(ie energies up to 2·5 GeV in the πN system) and beyond, and in many cases their spins and widths have been measured. One striking result of these analyses is that these higher mass resonances are usually broad and closely spaced so that in any given channel they may overlap with each other to simulate a smooth scattering amplitude.

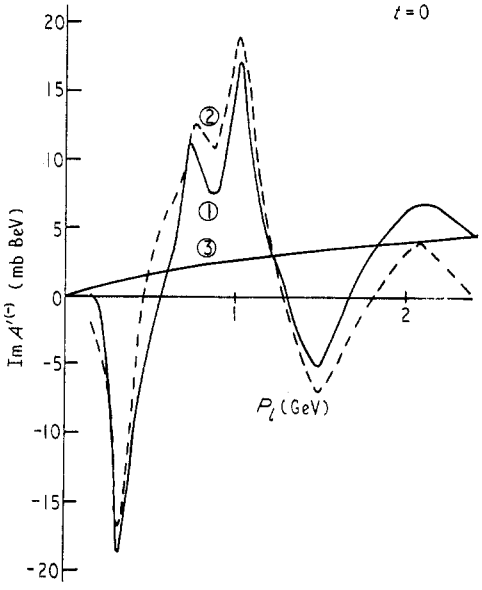

Figure 9. Comparison between the resonance (2) and Regge (3) contributions to Im $A'^{(-)}$ at $t = 0$. Curve (1) corresponds to the amplitude obtained from the total cross section difference (Dolen *et al* 1968).

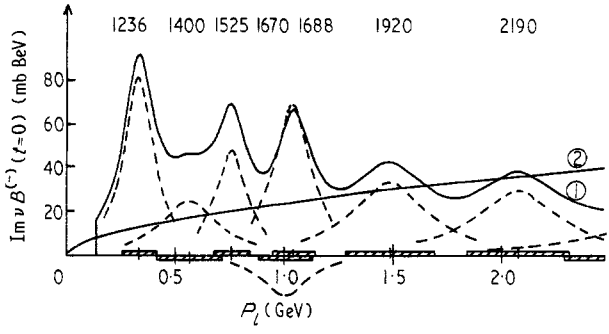

Figure 10. Comparison between the resonance (1) and Regge (2) contributions to Im $B^{(-)}$ at $t = 0$. The individual resonance contributions are shown by the broken lines (Dolen *et al* 1968).

As a specific illustration of this phenomenon, the two invariant amplitudes $A'^{(-)}$, $B^{(-)}$ for charge exchange scattering are shown in figures 9 and 10 against their resonant contribution. These illustrations are from Dolen *et al* (1968) who have obtained the resonance contributions from a Breit–Wigner type formula (see equation (3.2)), with the mass, width and spin parameters taken from the standard Rosenfeld table. These suggest that the s channel resonance contributions approximately saturate the charge exchange πN amplitudes over a pretty wide energy range. In contrast, similar analysis for the $A'^{(+)}$ and $B^{(+)}$ amplitudes, corresponding to vacuum quantum

number exchange, suggest a substantial background contribution over the same energy range (Harari and Zarmi 1969). We shall see later that the duality hypothesis requires such a background contribution for the vacuum exchange amplitudes (essentially to describe the pomeron exchange), while requiring resonance saturation for non-zero quantum number exchange. Note that the amplitude in this context refers to the imaginary part of the amplitude alone, with which we shall mostly be concerned in this section.

It should be emphasized, of course, that our knowledge of the resonance spectrum is too scanty to provide any convincing evidence either in favour or against the resonance saturation of scattering amplitudes. Even if all the resonances are detected and their spins and widths measured, there is an intrinsic ambiguity in the exact form of the Breit–Wigner expression when the widths involved are rather large, and the resulting resonant amplitudes (eg those of figures 9 and 10) will share this ambiguity. The results of these figures, nonetheless, provide a reasonable basis to hypothesize that the resonances saturate the scattering amplitudes (except for vacuum exchange) over a wide energy range so as to overlap with the leading Regge domain, and to look for *a posteriori* justification. This is essentially the duality hypothesis and the extent and the nature of this overlap define the various versions of this hypothesis. We shall discuss the hierarchy of these duality hypotheses in increasing order of severity.

3.1. Global duality

This hypothesis assumes the resonance contribution to describe the amplitude, in an average sense, over the sub-Regge energies. For πN scattering, for instance, this covers the 0–3 GeV range in laboratory momentum P_L ($P_L \simeq \nu$ for small t). It therefore only involves a marginal overlap between the resonance and the Regge pictures.

Under this hypothesis the FESR (equation (2.13)) reads

$$\int_{-N}^{-\nu_u} d\nu\, \nu^n \operatorname{Im} A_{\text{res}}(\nu) + \int_{\nu_s}^{N} d\nu\, \nu^n \operatorname{Im} A_{\text{res}}(\nu) = 2 \sum_i \gamma_i \frac{N^{\alpha_i+n+1}}{\alpha_i+n+1}. \tag{3.1}$$

With a standard Breit–Wigner formula for the resonance amplitude

$$A_{\text{res}} = \frac{\beta P_J(\cos\theta_s)}{s - m^2 + im\Gamma} \tag{3.2}$$

and a narrow resonance approximation for the energy denominator, equation (3.1) essentially reduces to

$$\sum_k \beta_k P_{J_k}(m_k, t)\, \nu^n(m_k) = 2 \sum_i \gamma_i \frac{N^{\alpha_i+n+1}}{\alpha_i+n+1} \tag{3.3}$$

where the summation k is over all the s and u channel resonances in the interval $-N \leqslant \nu \leqslant N$, whose mass, spin and coupling are denoted by m_k, J_k and β_k.

The spin of the external particles involve some non-essential complications which we ignore for the present.

One should note that analyticity and crossing play a crucial role in deriving the global duality relation (3.1) or (3.3), which make it possible to relate the leading Regge exchange to the contribution of resonances belonging to the sub-Regge

energy range. Equation (3.3) should hold for any even (odd) n, with the summation i corresponding to even (odd) signature trajectories.

However, this relation is only an approximate relation. Thus the prediction of a single moment sum rule (corresponding to a single value of n) is expected to be more reliable than those using several n values. Also the latter predictions are not exactly in the spirit of global resonance saturation. For varying n within a fixed cut-off N is essentially equivalent to varying N (with a fixed n), which presupposes resonance saturation in a somewhat more local sense. Nonetheless such predictions have been found very useful, particularly for studying the trajectory function α_i, and we shall discuss them along with those using single moment sum rules.

Dolen *et al* (1967, 1968) were the first to use the concept of global duality. They used this in an extensive study of the πN charge exchange amplitudes. It is illustrative to discuss some of these results. The charge exchange cross section is related to the invariant amplitudes $A'^{(-)}$ and $B^{(-)}$, corresponding to t channel helicity nonflip and flip, by

$$\frac{\mathrm{d}\sigma}{\mathrm{d}t} = \frac{m^2}{4\pi s^2}\left(|A'^{(-)}|^2 - \frac{t}{4m^2}\nu^2|B^{(-)}|^2\right) \tag{3.4}$$

at high energy and small t (see Singh 1963). The optical theorem gives

$$\sigma_{\pi^-\mathrm{p}} - \sigma_{\pi^+\mathrm{p}} = \frac{(2\sqrt{2})m}{s}\operatorname{Im} A'^{(-)}(t=0). \tag{3.5}$$

The s-channel helicity nonflip is also described by A' in this limit, whereas the flip amplitude is given by

$$A^{(-)} = A'^{(-)} - \nu B^{(-)}. \tag{3.6}$$

Both $A'^{(-)}$ and $\nu B^{(-)}$ have the asymptotic Regge behaviour ν^α and are antisymmetric under s-u crossing, so that they obey duality sum rules of the type

$$\int_{\nu_s}^{N} \operatorname{Im} A'^{(-)}_{\mathrm{res}}\, \nu^n \,\mathrm{d}\nu = \sum_i \gamma_i^a \frac{N^{\alpha_i+n+1}}{\alpha_i+n+1} \tag{3.7}$$

and

$$\int_{\nu_s}^{N} \operatorname{Im} B^{(-)}_{\mathrm{res}}\, \nu^{n+1} \,\mathrm{d}\nu = \sum_i \gamma_i^b \frac{N^{\alpha_i+n+1}}{\alpha_i+n+1} \tag{3.8}$$

for even n.

3.1.1. Resonance correlation. One application of global duality is to use the leading Regge (in this case ρ) parameters on the right hand side in order to correlate the low energy resonance couplings on the left. Without going into detail one can see qualitatively the success of such a scheme. The high energy charge exchange cross section suggests a significantly larger flip residue of ρ compared to the nonflip, which also agree with the nuclear form factor estimates. Since these residues are built up from the same set of s channel resonances, one should expect from (3.7) and (3.8) that these contributions should be strongly correlated, so as to reinforce each other for νB and mutually cancel for the A' amplitude. This, indeed, is the case as we see from figures 9 and 10. These figures correspond to the left hand side of (3.7) and (3.8) for the lowest moment ($n = 0$) case.

3.1.2. Regge parameters. The second, and perhaps the more important application of these duality relations is to estimate the Regge parameters on the right hand side. For instance the trajectory and residue functions can be calculated by feeding in the baryon resonance parameters on the left hand side of (3.7) and (3.8). This would yield, in particular, the ρ mass and coupling constants. The flip amplitude $B^{(-)}$ is

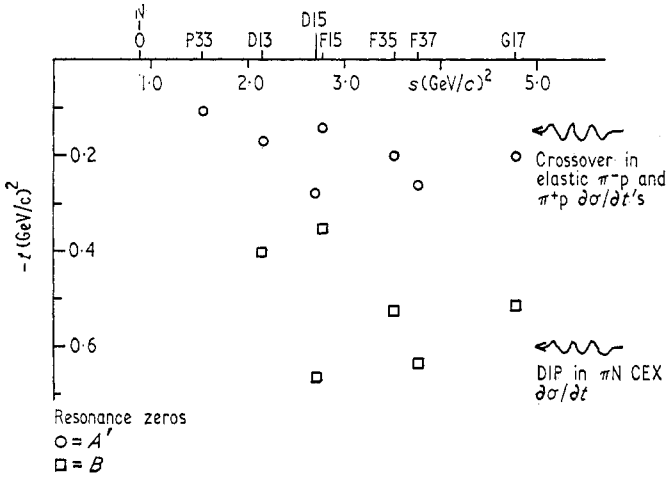

Figure 11. The prominent π–N resonances have zeros in A' near $t \simeq -0{\cdot}2$ (the cross-over region) and in B near $t \simeq -0{\cdot}5$ (the dip region) (Berger and Fox 1970).

the more suitable for this purpose. High energy scattering data suggest this amplitude to have negligible contamination from cuts, so that the right hand side of (3.8) contains a single term

$$\gamma_\rho^b \frac{N^{\alpha_\rho+n+1}}{\alpha_\rho+n+1}.$$

Thus the ratio of the left hand integral for $n = 0$ and $n = 2$ determines the trajectory α_ρ. The trajectory so evaluated (Dolen *et al* 1968) gives

t	$\alpha(t)$
m_ρ^2	$1 \pm 0{\cdot}3$
0	$0{\cdot}4 \pm 0{\cdot}2$
$-0{\cdot}2$ GeV²	$0{\cdot}3 \pm 0{\cdot}3$

and passes through zero in the t-range $-0{\cdot}3$ to $-0{\cdot}6$ GeV². This agrees well with the trajectory obtained either from the Chew–Frautschi plot or from the high energy data. Similarly the residue function, calculated from the lowest moment sum rule, has been shown (Dolen *et al* 1968, Barger and Phillips 1969a, Harari and Zarmi 1969) to agree very well with the high energy estimates in the negative t region and with the on-shell coupling constant at $t = m_\rho^2$. In particular the zeros of the baryon resonance terms (associated with the first zeros of the corresponding Legendre functions), as displayed in figure 11 (Berger and Fox 1970), all lie in the t range of $-0{\cdot}4$ to $-0{\cdot}6$ GeV². This means that the resulting residue γ_ρ^b must also have a zero in the same region, especially as the resonance contributions are all

additive. This agrees remarkably with the wrong-signature zero that is expected on theoretical grounds and confirmed by the high energy data.

Similarly the zeros of the baryon resonance terms in the nonflip amplitude occur mostly in the t range of $-0{\cdot}1$ to $-0{\cdot}3$ GeV^2, which would lead to a zero in the leading Regge contribution in this interval. A cross-over between the high energy π^-p and π^+p differential cross sections near t about $-0{\cdot}2$ GeV^2, indeed, suggests such a zero in the leading Regge contribution to Im$A'^{(-)}$. On the basis of factorization constraints it is generally believed that this zero does not arise from a vanishing of the ρ residue, but due to a cancellation between the ρ pole and the ρ-P cut terms. We shall come back to this point at the end of this section. It suffices to point out here that such a zero will move very slowly with energy, due to the almost identical energy dependence of the two terms. Therefore, such a zero will be phenomenologically indistinguishable from a residue zero in the analysis of Im$A'^{(-)}$.

3.1.3. Bootstrap. The interrelation between the resonance and Regge contributions gives a linear bootstrap scheme if the same trajectory appears in the formation (s) and the exchange (t) channels. Here the trajectory α and residue γ functions can be determined through self-consistency, from relations of the type (3.3). Such relations cannot fix the overall normalization of the residue function in which they are linear. Besides, one does not expect to match the trajectory and residue functions over the same range of four momentum square, since the latter is negative or marginally positive on the right hand side (ie t), and corresponds to large positive values on the left (ie s). With an analytic parameterization of the trajectory and residue functions in terms of the four momentum squared, however, they can be completely determined by matching the two sides of the duality relation, apart from the overall normalization.

Such a self-consistency scheme for the meson trajectory in the s and t channels was first investigated by Mandelstam (1968) in the context of baryon–antibaryon scattering with some success. The most remarkable result in this line, however, was that of Ademollo *et al* (1967) on the ρ bootstrap in $\pi\pi \to \pi\omega$. For this reaction there is only one invariant amplitude and all the three channels are identical. Moreover the quantum number considerations single out ρ from amongst the known meson resonances. By setting the cut-off N above the g meson mass (ie the next recurrence of ρ), one obtains a duality relation like (3.3), with the ρ and g couplings on the left and the ρ trajectory residue on the right. With a simple parametric representation for the trajectory and residue functions, self-consistency was achieved over a large range of t. Also the ρ parameters, so obtained, had the right phenomenological features. The self-consistency was lost when the scheme was repeated by increasing N to include still higher recurrences of the ρ. However, it could be restored by adding low spin mesons at the mass of the ρ meson and its higher recurrences. The plausibility for such lower spin partners had been recognized for some time and was referred to as the daughter structure. The above investigation demonstrated that a linearly rising ρ trajectory cannot be self-sustaining, but a self-sustaining scheme can be achieved with a linearly rising ρ together with its daughter structure. It is worth noting that this result led subsequently to the construction of the famous Veneziano model.

3.1.4. Exoticity constraints. Writing the global duality relation for exotic channels gives useful information on the internal symmetry of the Regge trajectories (Roy

and Suzuki 1969). To illustrate this point, we consider some specific examples. The elastic $K^0\Delta^{++}$ amplitude is exotic, both in the s and the u channels. Hence by (2.13) and (3.3) the even and odd signature Regge exchanges in the t channel must separately vanish. This means that the vector and tensor trajectories should mutually cancel. Moreover, using the duality relation (3.3) for two different moments would require the cancellation to occur amongst a degenerate set of vector (so also tensor) trajectories. This implies that the trajectories must either occur in degenerate isoscalar–isovector pairs so as to cancel in the $K^0\overline{K^0}\to\Delta^{++}\overline{\Delta^{++}}$ channel, or else must decouple from this channel. The Chew–Frautschi plot for the vector and tensor nonets shows degenerate ρ–ω and f–A_2, whereas ϕ and f occur singly. Thus ϕ and f should decouple from this channel (and similarly from the $\pi^+\pi^-\to\Omega\overline{\Omega}$ channel). The ϕ, f decoupling from the non-strange meson and baryon vertices is a well-known result of the quark model with ideal mixing, and is also supported experimentally. Since the pomeron cannot have an isovector partner it must either decouple from the above reactions or else be dual to the non-resonant background. The first alternative, corresponding to an asymptotically vanishing σ_T, is unacceptable for many theoretical and phenomenological aspects of diffraction scattering. Thus the pomeron must be dual to the non-resonant background. We shall come back to this point in the context of semilocal duality, on the basis of which this assignment was first suggested.

The A_2–f cancellation requirement, together with the SU(3) coupling relations for the tensor octet, gives the f–f' mixing angle by

$$\tan\theta = \frac{1}{\sqrt{2}}. \tag{3.9}$$

The ρ–ω cancellation on the other hand is identically satisfied by the SU(3) symmetric vector couplings, irrespective of the mixing angle. This is because the SU(3) singlet vector meson cannot couple to the $K\bar{K}$ channel. However, applying similar considerations to the reaction $K^0\Delta^{++}\to K^{*0}\Delta^{++}$, leads to an identical angle for ω–ϕ mixing. It should be noted that the observed vector and tensor meson masses and the Gell-Mann–Okubo mass formula also leads to the same mixing angle.

Of course the above mixing angle as well as the ϕ, f' decoupling condition and the ρ–ω and A_2–f degeneracies are standard results of the quark model. They constitute the well-known quark nonet scheme. Similarly the absence of resonances in the exotic channel is a part of this quark model scheme, as we saw in the last section. However, the significant aspect of duality is the way it relates the above set of results to the absence of exotic resonances without involving any assumption about the quarks.

Applying similar considerations to baryon–antibaryon scattering leads to a radically new result; namely, there must be exotic resonances in baryon–antibaryon channels. Consider for instance the charge exchange reaction $\Delta^+\bar{\Xi}^+\to\Delta^{++}\bar{\Xi}^0$. Here the u channel is exotic being a di-baryon state, and the s channel is also exotic due to double charge. However, the t channel vector (or tensor) contribution cannot vanish, since only ρ (or A_2) is exchanged, therefore there should be s channel resonances to be dual with the exchanged ρ contribution. Experimentally very little is known about the resonance structure in the baryon–antibaryon channels. The observed resonance spectrum and the duality results for meson–meson and meson–baryon scattering suggest, however, that even if such resonances are

present their coupling to the mesonic channels must be very weak. Finally it should be noted that this exotic resonance prediction follows from a single moment rule and is therefore a consequence of global duality, even in a strict sense. Historically, however, they were first obtained on the basis of the semilocal version of duality (Rosner 1968).

3.2. Semilocal duality

The hypothesis of resonance saturation in the sub-Regge region (0 to N) is now extended to cover a higher energy range (N') so that there is a substantial overlap between the resonance and the leading Regge descriptions. Moreover the resonance saturation is assumed to be somewhat more local. For instance, the amplitude in the interval N to N' is assumed to be averaged by the resonance contributions over this interval; and such an averaging by the local resonances is assumed to hold for several intervals of energy (ie several values of N'). From the general shape of the resonance contribution to the imaginary part of an amplitude (see figure 10) we see that such a local averaging should be very reasonable as long as the interval is large—a few GeV say. In particular it is reasonable to assume that the resonances from the negative ν region (u channel resonances) do not affect the amplitude in the $\nu > N$ region, as long as one deals with the imaginary part only. This assumption is vital to the results of semilocal duality.

The overlap between the t channel Regge and s channel resonance contributions in the interval N to N' can be expressed as

$$\int_N^{N'} \mathrm{Im}\, A_{\mathrm{res}}\, \mathrm{d}\nu = \sum_i \frac{\gamma_i}{\alpha_i + 1}(N'^{\alpha_i+1} - N^{\alpha_i+1}) \tag{3.10}$$

where the summation i is over both even and odd signature Regge exchanges. This relation evidently does not involve any considerations of analyticity or crossing. In terms of predictive power equation (3.10) is much stronger than the global duality relation (3.1) since it relates the t channel Regge exchange to s channel and u channel resonances separately. It is, in fact, the most widely used version of phenomenological duality.

3.2.1. Exchange degeneracy and two-component duality. The even and odd signature Regge contributions should cancel each other in equation (3.10) whenever the s channel is exotic. Moreover this cancellation must occur separately for each set of degenerate Regge trajectories, since (3.10) should hold for several intervals of energy. This means that opposite signature Regge trajectories should occur in degenerate sets. This is the exchange degeneracy (EXD) result, mentioned in the last section.

Since the pomeron does not (and on general theoretical grounds should not) have an exchange degenerate partner, it would have been required to decouple from such exotic channels as the elastic K^+p or pp scattering, which is inadmissible in view of their large asymptotic cross sections (figure 12). This has led Freund (1968) and Harari (1968) to postulate the two-component theory of duality, where the pomeron is dual to the background and all the 'normal' Regge trajectories are dual to the s channel resonances, as mentioned earlier. A number of interesting EXD results amongst the latter follow from considering exotic channels.

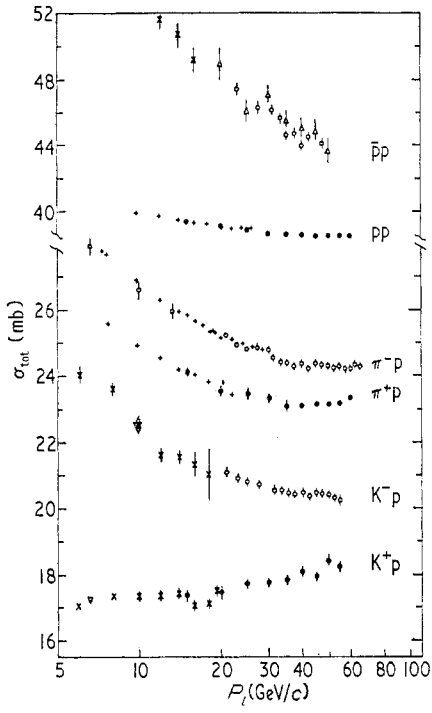

Figure 12. Total cross sections of $\pi^{\pm}$ p, $K^{\pm}$ p, pp and $\bar{p}$p as functions of p_{lab}. K^+ n and pn data are indistinguishable within error bars from K^+ p and pp data. The pomeron term seems to show a slight increase for K^+ p around 50 GeV/c and for pp around 1000 GeV/c (not shown).

3.2.2. Weak exchange degeneracy. A number of exotic channels in meson–meson scattering are listed below, alongside the possible Regge exchanges.

Exotic channel	Regge pole exchange
$\pi^+\pi^+ \to \pi^+\pi^+$	$\rho, f; f'$
$\pi^+ K^+ \to \pi^+ K^+$	$\rho, f; f'$
$K^+ K^0 \to K^0 K^-$	ρ, A_2
$K^+ K^+ \to K^+ K^+$	$\rho, A_2; \omega, f; \phi, f'$
$\pi^+ K^+ \to K^+\pi^+$	K*, K**
$\pi^+\rho^+ \to \rho^+\pi^+$	$\omega, A_2; \phi$

The only EXD solution to these channels consistent with the observed degeneracy breaking between ω and ϕ (or f and f') is

$$\begin{aligned} \alpha_\rho &= \alpha_{A_2} = \alpha_f = \alpha_\omega \\ \alpha_{K^*} &= \alpha_{K^{**}} \\ \alpha_\phi &= \alpha_{f'}. \end{aligned} \tag{3.11}$$

Such an EXD scheme between the trajectory functions is usually called weak EXD. The weak EXD relation given by equation (3.10) is satisfied extremely well by the observed vector and tensor trajectories (figure 13).

3.2.3. Strong exchange degeneracy. The EXD condition between the residue function is referred to as strong EXD. The strong EXD relation can be tested better in meson–baryon or baryon–baryon scattering, where one has direct experimental

information on the scattering amplitudes. We should only point out two significant results of the last subsection, which also follow directly from the above list of reactions (Chiu and Finkelstein 1968). The exotic channels $\pi^+\pi^+ \to \pi^+\pi^+$ and $\pi^+\rho^+ \to \rho^+\pi^+$ require ϕ and f' decoupling from $\rho\pi$ and $\pi\pi$ channels respectively.

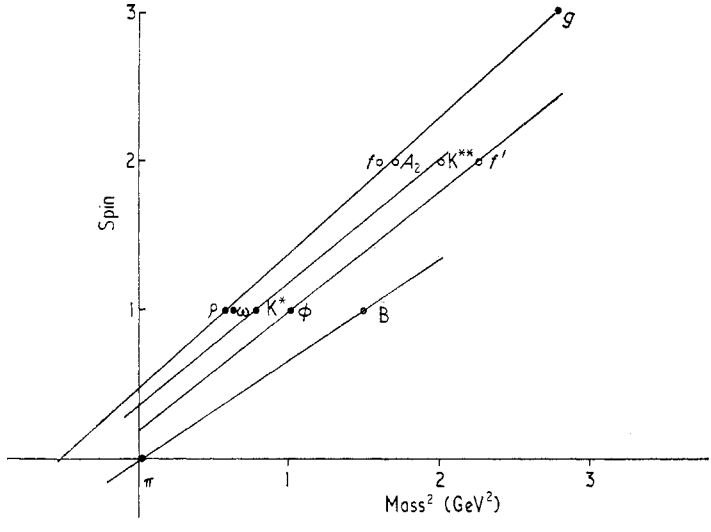

Figure 13. Exchange degenerate meson trajectories.

Moreover, the four top channels give, through factorization,

$$\begin{aligned} \gamma_{\rho K^+K^-} &= \gamma_{\omega K^+K^-} \\ \gamma_{fK^+K^-} &= \gamma_{A_2K^+K^-} \end{aligned} \tag{3.12}$$

which are identical to the SU(3) coupling relation with the standard ω–ϕ (or f–f') mixing angle given by

$$\tan\theta = \frac{1}{\sqrt{2}}.$$

The strong EXD relations for the exotic channels $K+p \to K+p$ or $pp \to pp$ suggest that the 'normal' Regge contribution to the imaginary part of these amplitudes (or to the corresponding total cross section σ_T by (2.7)) should vanish. Then the total cross section in these cases should be given entirely by the pomeron term and should therefore remain constant over the entire Regge domain. In contrast the σ_T for the non-exotic channels K^-p or $\bar{p}p$ should approach the asymptotic value from above, since the resonance terms, generating the 'normal' Regge part, should all be positive. Moreover the differences $(\sigma_T^{K^+p} - \sigma_T^{K^+n})$ and $(\sigma_T^{pp} - \sigma_T^{pn})$ should vanish over the entire Regge domain in contrast to the non-exotic case. All these results agree extremely well with the total cross section data (figure 12).

3.2.4. Wrong-signature zeros. Another interesting consequence of strong EXD is the wrong-signature zero (WSZ), described in the last section. For instance the A_2 residue in $K^+n \to K^0p(\gamma_{A_2})$ should vanish at $t \simeq -0{\cdot}5$ GeV^2, corresponding to $\alpha_{A_2} = 0$, in order that the amplitude (see 2.5*a*) does not diverge in the scattering region. Therefore by strong EXD γ_ρ should vanish at the same point, and by SU(3)

this should propagate to the ρ residue in $\pi^- p \to \pi^0 n$. Since $\alpha = 0$ is a wrong-signature point for ρ, the amplitude (equation 2.5*a*) should vanish at this point. Such a zero is, indeed, a very well-known feature of the $\pi^- p$ charge exchange scattering data.

3.2.5. Exchange degenerate baryons. Duality considerations applied to exotic meson–baryon scattering also lead to exchange degeneracy between baryon trajectories. For instance duality in backward $K^+ p$ scattering (ie $K^+ p \to pK^+$) leads to exchange degeneracy between the hyperon trajectories (Schmid 1969, Barger and Michael 1969). Some exchange degenerate sequences can be readily recognized from the Chew–Frautschi plot of figure 14, like the $\Lambda(1115, \frac{1}{2}^+)$–$Y_0^*(1520, \frac{3}{2}^-)$ sequence. The situation for the baryon trajectories, however, is not as clear as the meson case. We shall discuss this situation further, together with the baryon–antibaryon scattering case, in the next section.

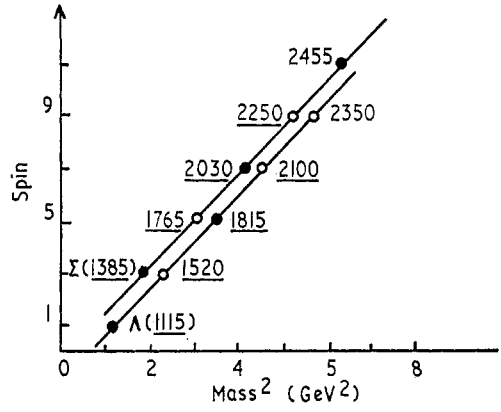

Figure 14. Exchange degenerate baryon trajectories.

3.3. Local duality (high energy version)

The resonance saturation is now assumed to be over the same range of energy as in the semilocal version, but the saturation is assumed to be much more local. This means that over any small subsection of the interval N to N', whose width is given by the typical separation between the consecutive resonance masses, the amplitude is approximated by a single resonance contained in the subsection. Note also that, although this subsection is expected to contain a tower of degenerate resonances (the daughter structure), the dominant contribution is assumed to come from a single spin state. Thus one assumes a local overlap between the t channel Regge exchange and the local resonance contribution, throughout the range N to N'. But the leading Regge exchange is characterized by fixed t structure (eg the wrong-signature zero), whereas a typical s channel resonance term has a structure given by its spin and $\cos\theta$ (eg by $P_j(\cos\theta)$ of equation (3.2)). Thus the assumed overlap implies a strong correlation between the mass and the spin of the dominant resonances.

3.3.1. Peripheral resonances. The above correlation has been analysed in detail for the πN charge exchange scattering. Here the dip in the cross section comes from a zero in the amplitude A around $t \simeq -0{\cdot}5$ GeV^2 and is associated with the wsz of the

ρ pole exchange. A and A' are the s channel helicity flip and nonflip amplitudes. According to a well-known identity, the Legendre function associated with a spin j resonance can be approximated by the Bessel function $J_1[(j+\frac{1}{2})\sin\theta/2]$ and $J_0[(j+\frac{1}{2})\sin\theta/2]$ in the flip and nonflip case, for large j. Thus a resonance of spin j and mass W_R has a zero in A at

$$(j+\tfrac{1}{2})\sin\tfrac{1}{2}\theta \simeq (j+\tfrac{1}{2})\frac{\sqrt{-t}}{W_R^2} = 3{\cdot}8 \tag{3.13}$$

associated with the zero of $J_1(x)$ at $x = 3{\cdot}8$. In order to match with the wrong signature zero at $t \simeq -0{\cdot}5$ GeV^2, the dominant resonances must be on a line

$$(j+\tfrac{1}{2})W_R^{-1} \simeq 5 \text{ GeV}^{-1} = 1 \text{ fermi}. \tag{3.14}$$

These are called peripheral resonances, since they correspond to

$$j(2q_R)^{-1} \simeq 1 \text{ fermi} \tag{3.15}$$

(q_R is the s channel centre of mass system momentum at the resonance mass), which is equivalent to scattering from the periphery of a disc of constant radius $\simeq 1$ fermi.

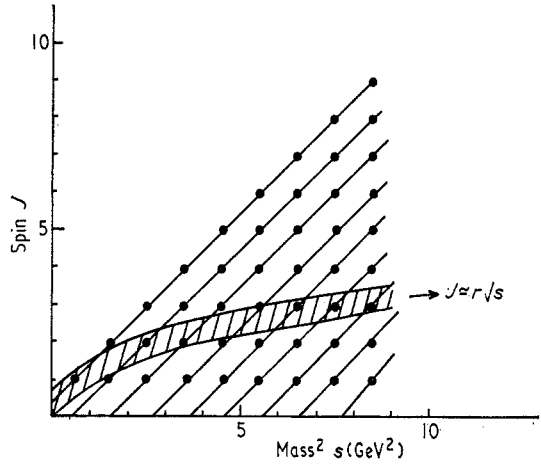

Figure 15. Schematic representation of peripheral resonances. Although the resonances are expected to lie on linear trajectories accompanied by sets of daughters, the prominent ones for the elastic channel are assumed to lie on the parabola $J \simeq r\sqrt{s}$. Such a resonance pattern would correspond to scattering from the periphery of a disc of radius r.

Thus, although the nucleon resonances are supposed to lie on linear trajectories

$$j \propto s_R \tag{3.16}$$

accompanied by the lower spin daughters, the prominent elastic resonances, according to this hypothesis, should be on a parabola

$$j \propto \sqrt{s_R}. \tag{3.17}$$

This is shown graphically in figure 15.

Of course, it is by no means essential to have a peripheral resonance structure (equation (3.17)) in order to reproduce the fixed t zeros. Parent and daughter resonances lying on linear trajectories could alternatively be correlated so that they reproduce the wrong-signature zero at $t \simeq -0{\cdot}5$ GeV^2 as in §6. However, if the

dominant resonances occur on a peripheral curve, this would imply an interesting correlation between the zeros of the helicity flip and the nonflip amplitudes. For instance, the peripheral nucleon resonances of equation (3.14) imply a zero in the A' amplitude at $t \simeq -0{\cdot}2$ GeV^2, corresponding to the first zero of the $J_0(x)$ at $x = 2{\cdot}4$. Indeed such a zero is confirmed by the $\pi^{\pm}$–p cross-over phenomenon, as we mentioned earlier.

On the basis of the above success, local duality has been invoked (Kugler 1970, Harari 1971) to suggest a peripheral imaginary part as a general feature of any scattering amplitude, apart from the pomeron component. Such a system is often referred to as geometrical duality. It seems to have reasonable support from high energy data.

3.4. Local duality (low energy version)

In this version a local (or sometimes semilocal) overlap is assumed between the resonance and the leading Regge descriptions, even over the sub-Regge domain ($0 < \nu > N$). From a theoretical standpoint this is perhaps the least reliable version of duality. For even if the resonance saturation were good everywhere there is little *a priori* ground to assume that the leading Regge terms describe the low energy amplitude, in any average sense. In particular the s channel integral

$$\int_0^N \mathrm{Im}\, A \, \mathrm{d}\nu \tag{3.18}$$

is expected to have contributions not only from the leading Regge exchanges (ie those in equation (3.10)), but also from certain wrong signature fixed poles, which do not affect the high energy scattering amplitudes (Schwarz 1967). Only in the specific case of an odd crossing amplitude does this latter contribution drop out as in equations (3.7) and (3.8). In certain dual models like the Veneziano model such fixed pole contributions are expected to be significant when neither of the two resonance channels (s and u) is exotic.

Nonetheless, considerable work has been done to check phenomenologically if the leading Regge exchange does describe the low energy resonances, either locally or through integrals like (3.18). The success here has been rather mixed.

First of all, the fixed t structures of the leading Regge exchange would suggest the dominant s channel resonances to be peripheral, as described earlier. A number of the elastic resonances in the πN channel are, indeed, seen to be peripheral. One can see this directly from figure 11 where individual resonances are seen to possess the fixed t zeros. A similar systematics is seen to hold for $\bar{K}$N scattering as well (Fukugita and Inami 1972).

3.4.1. Argand loops. A more ambitious programme for studying local duality was by projecting out a partial wave of the Regge amplitude and then analysing it on the phase plot as a function of energy (Schmid 1968).

In the phase plot, one plots the imaginary part of the partial wave amplitude versus its real part at various energies. While passing through a resonance mass, such a plot is expected to describe a circle anticlockwise with the top point of the circle being reached at the resonance mass $s = m^2$. One can deduce these features directly from the resonance amplitude of equation (3.2). These are the so-called Argand loops.

The partial waves projected out of the ρ-exchange term have been shown to describe such loops in the phase plot (Schmid 1968, Chiu and Kotanski 1968a,b). In fact, one can in this way generate a set of nucleon resonances and match it with the 1920–2190–2920 series (Schmid 1968). The relevance of such loops to actual resonances, however, is very much an open issue (see eg Collins *et al* 1968). Apart from certain theoretical problems, the generated resonances seem to be too broad and globally displaced in mass compared to the actual ones.

If the integral (3.18) is to be described by the leading t channel Regge exchanges then the resonance contribution to such an integral should mutually cancel if the amplitude A has an exotic t channel. Such a cancellation amongst the low energy resonances has been observed in the $\pi^- p \to \pi^+ \Delta^-$ amplitude (Kernan and Sheppard 1969), but one also has counter examples like $K^- p \to \pi^+ \Sigma^-$ (Ferro-Luzzi *et al* 1971) or $\pi^+ \pi^- \to \pi^- \pi^+$ where such cancellations do not seem to occur.

We do not intend to make a critical evaluation of the above phenomenological successes and failures. We should simply remark that the failures can mostly be traced to the fixed pole effects (Roy 1971). With the correct crossing amplitude, the leading Regge terms seem to provide a good semilocal average of the low energy resonances.

3.5. Concluding remarks

3.5.1. Pole–pole against pole–cut duality. The first remark concerns the nature of the leading Regge exchange. To start with, the duality hypothesis was postulated between the resonance and the Regge pole contributions. On a phenomenological level, however, certain features of the scattering amplitude seem to be interpreted more naturally as pole–cut interference effects rather than with pole terms alone. One such effect is a zero in $\mathrm{Im}\, A'^{(-)}$ at $t \simeq -0{\cdot}2$ GeV^2—the cross-over zero—which is associated with the ρ and ρ–P cut cancellation. We have seen earlier that the dominant resonance contributions to $A'^{(-)}$ share this zero. Similarly the forward photoproduction amplitude shows a sharp spike, presumably associated with the π pole and the π–P cut interference, that seems to be shared by the resonance contribution to the amplitude as well.

It seems more natural, therefore, that the resonance contributions are dual to the leading Regge contribution, containing both the pole and the pole–pomeron cut. However, this may not affect most of the results based on factorization, since it should still work over a certain range of t, where the pole is expected to dominate. Moreover, it has been argued on the basis of the SU(3) singlet and the imaginary nature of the pomeron that the SU(3) and the EXD properties of Regge pole terms are likely to hold for the corresponding Regge–pomeron cut as well (Barger and Phillips 1969b).

On a more basic mathematical level such an association of resonance poles with Regge cuts seems hard to interpret, particularly for large cut terms. From analyticity considerations, it is simpler and perhaps more natural to associate resonance poles with poles in the angular momentum plane, and the existing formulations of mathematical duality (§ 6) always start with functions having such pole–pole duality. Of course unitarization prescriptions have been suggested, which develop a perturbation series in the above function to describe the physical amplitude. In general the higher order terms contain parts having resonance poles dual with Regge cuts and also ones with Regge poles dual with background. However, the

higher order terms are expected to be small, according to the basic hypothesis of duality. In particular, it seems very implausible that one can generate large Regge cut terms without at the same time breaking the resonance dominance in the energy plane. However, one cannot reach a definite conclusion on this subject so long as one does not have a reliable model for Regge cuts or even for the pomeron singularity.

3.5.2. Approximate and exact duality. The various types of equalities between the resonance and the Regge contributions described in this section must all be re-regarded as approximate equalities only. If any of these equalities were exact it would have been superfluous to postulate so many versions of duality—ie all versions could be derived starting with global duality. One can see this directly from equations (3.7) and (3.8). If these were exact equalities consistency requirements between high and low values of n would require the two sides to match locally, but since the relations are only approximate, the resulting consistency conditions need not hold. (For example the approximate equalities $90 \simeq 100$ and $98 \simeq 100$ should not imply $2 \simeq 10$.) Hence the semilocal or local versions of duality must be regarded as separate hypotheses.

It is fairly straightforward to see that a finite number of resonances cannot be described exactly by a finite number of Regge poles. Apart from the fact that the latter would not have any second sheet poles unlike the resonances, the disagreement is obvious even in the physical region. The resonance contributions to equation (3.3), for instance, would give a polynomial t behaviour, whereas the Regge contributions on the right hand side are exponential functions of t. Thus the two descriptions may be expected to match only approximately and that too only over a limited t range. Phenomenologically this range is roughly taken to be $0 > t > -1$ GeV^2, where one has most direct evidence of resonance saturation. It is possible, however, to achieve a rigorous equality between the two descriptions by invoking an infinite sequence of lower lying Regge poles—the daughters—as we shall see in § 6.

3.5.3. Interference model. Finally we discuss the so-called interference model, which provides an alternative to duality and historically precedes it. In this model the scattering amplitude in the sub-Regge region was assumed to be given by the sum of the resonance and the leading Regge contributions (Barger and Cline 1968). This would imply that the resonance contributions to any finite energy sum rule (eg equation (2.13)) should mutually cancel out to zero. We have seen from figure 10, that this is far from being the case, at least for the charge exchange amplitude $B^{(-)}$. Moreover, such a cancellation would be very implausible for the elastic amplitudes, since the individual resonance contributions here are all expected to be positive on the basis of unitarity. It has, however, been pointed out that the positivity criterion need not hold if there is a large background, since the resonance component need not be unitary by itself. In particular it is possible to define negative resonance contributions, even for elastic amplitudes, in this way (Donnachie and Kirsopp 1969). Nonetheless, it is fair to say that there is little positive evidence in the resonance data which would be suggestive of such a cancellation. Moreover, if one assumes the interference model, then many striking results of duality like EXD have to be dismissed simply as accidental phenomena. Thus, although there is no fundamental physical principle which would rule out the interference model in favour of duality, the experimental data seem to support the latter overwhelmingly.

4. Dual classification of hadron spectrum

This section surveys the application of duality in classifying the meson and baryon spectra. These classifications are based on the semilocal version of duality as described in the last section. For instance, the absence of resonances in a certain channel implies a correlation between trajectories of opposite signatures (and often with different internal quantum numbers) in the cross channel—ie exchange degeneracy. Thus the absence of resonances in the $\pi^+\pi^+$ channel provides a correlation between the vector trajectory ρ with isospin 1 and the tensor trajectory f with isospin 0. This result can be formally derived by using the isospin crossing matrix in $\pi\pi$ scattering

$$\begin{vmatrix} A_s^0 \\ A_s^1 \\ A_s^2 \end{vmatrix} = \frac{1}{6} \begin{vmatrix} 2 & 6 & 10 \\ 2 & 3 & -5 \\ 2 & -3 & 1 \end{vmatrix} \begin{vmatrix} A_t^0 \\ A_t^1 \\ A_t^2 \end{vmatrix}. \tag{4.1}$$

The exoticity condition A_s^2 (resonance) $= 0$ gives a linear relation amongst the t channel Regge contributions in A_t^0, A_t^1 and A_t^2. Since there are no isospin 2 Regge poles, this reduces to a relation between A_t^0 and A_t^1. Moreover this relation, as in equation (3.10), must be satisfied independently for each set of degenerate trajectories. There can be four members in each set—positive and negative signature trajectories, each with isospin 0 and 1. However, the positive signature isovector (eg A_2) and the negative signature isoscalar (eg ω) cannot couple to the $\pi\pi$ channel by charge conjugation parity. Thus the trajectories in the $\pi\pi$ channel should always occur in a degenerate set of two isospin multiplets—a positive signature isoscalar (eg f) and a negative signature isovector (eg ρ)—with residues related by one linear homogeneous relation. This makes it an exactly determined set, apart from the overall normalization of the residue.

The same procedure can be extended to the case of SU(3), where one substitutes the SU(3) crossing matrices and multiplets in equation (4.1). Thus the absence of resonances in certain SU(3) multiplets would provide degeneracy conditions amongst the positive and negative signature Regge trajectories belonging to different SU(3) multiplets in the cross channel. Duality and exoticity conditions, therefore, would lead to a super multiplet structure, consisting of a degenerate set of several SU(3) multiplets with related residues. In this respect the role of duality is comparable to that of a higher symmetry scheme (eg SU(6)).

The above procedure has been applied extensively to meson–meson, meson–baryon and baryon–antibaryon scattering (Mandula *et al* 1969a, Mandula *et al* 1969b, Capps 1969a,b). The resulting degeneracy relations amongst the SU(3) multiplets of mesons and of baryons provide some very interesting comparisons with the observed particle spectra. A detailed account of these results is contained in a review article by Mandula *et al* (1970). We shall presently discuss the essential features of these analyses. We shall omit the details of the various SU(3) crossing matrices and the resulting degeneracy equations. Nonetheless, we shall try to make the results plausible at each stage, using mostly qualitative considerations.

4.1. Meson–meson scattering

4.1.1. Pseudoscalar–pseudoscalar scattering. Let us consider first the scattering of pseudoscalar octets (P), where only natural parity exchanges can contribute. By particle–antiparticle symmetry in this case all the three channels consist of the five

independent SU(3) states

$$8(\times)8 = 1(+)8_{SS}(+)8_{AA}(+)(10(+)\overline{10})(+)27. \qquad (4.2)$$

Here 8_{SS} and 8_{AA} are the two independent octet states, coupling symmetrically (D type) and antisymmetrically (F type) to the pseudoscalar octets. The decouplet states 10 and $\overline{10}$ are mutually related by charge conjugation.

One easily sees from the SU(3) analogue of the s-t crossing relation (4.1) that the absence of s channel resonances in the $(10+\overline{10})$ and the 27 states gives two linear homogeneous relations which must be satisfied by a degenerate set of t channel trajectories. *A priori* there could be six independent trajectories corresponding to 1, 8_{SS} and 8_{AA} states for either signature. However, the trajectories must have a charge conjugation parity $C = +C_1 C_2$ for the singlet and the symmetric octet couplings and $C = -C_1 C_2$ for the antisymmetric octet coupling, where C_1 and C_2 are the C parities of the two external octets. For pseudoscalar–pseudoscalar scattering $C_1 = C_2 = +1$. Thus only three of the six t channel trajectories can couple, namely the positive signature (tensor with $C = +1$) trajectory belonging to the singlet and the symmetric octet states and the negative signature (vector with $C = -1$) belonging to the antisymmetric octet. Therefore with two linear homogeneous relations this reduces to an exactly determined set of three degenerate trajectories, which are the vector octet with F type coupling, the tensor singlet and the tensor octet with D type coupling.

4.1.2. Pseudoscalar–vector and vector–vector scattering. Next consider the s channel pseudoscalar octet–vector octet scattering PV→VP, where both natural and unnatural parity exchanges contribute. Owing to the linear nature of the crossing relations, one can separate the natural and unnatural parity exchanges in the t channel and apply identical duality considerations to each. Then for the natural parity exchange the situation is very similar to the previous case, except that here $C_1 = -C_2 = +1$. Thus the solution here consists of a degenerate set of the tensor octet with F type coupling, the vector octet with D type coupling and a vector singlet. Therefore the combined duality solution to the pseudoscalar–pseudoscalar and the pseudoscalar–vector scattering implies that the natural parity meson multiplets must always occur in a degenerate set of four with mutually related residues—ie as exchange degenerate vector and tensor nonets. Alternatively, of course, one could have a bigger (and clumsier) solution where the two degenerate sets of three do not overlap. Here, for instance, the tensor octet of the PP channel would be required to decouple from the PV channel and vice versa. Fortunately, however, the observed meson spectrum rules out these alternative solutions.

Similarly the combined duality constraints for unnatural parity trajectories in PV→VP and VV→VV imply that they too must occur in degenerate sets of four comprising octets and singlets of positive and negative signature. This result holds separately for natural C parity ($C = (+1)^J$) and unnatural C parity ($C = (-1)^J$) mesons. Consequently the nonet of pseudoscalar trajectories ($\pi, \mathrm{K}, \eta, \eta'$) are required to be exchange degenerate with a nonet of axial vector trajectories with negative C parity. The B(1235), H(990) and Q(1320), which would roughly overlap with the pseudoscalar nonet trajectories on a Chew–Frautschi plot, are usually identified as members of this axial vector nonet. Finally the observed axial vector mesons with unnatural C parity (eg $A_1(1070)$ and $D(1285)$) should also form a nonet, and be degenerate with a nonet of positive signature trajectories (presumably axial tensors) to complete a duality set. However, the identification of this last

duality set with the observed meson spectrum is still very incomplete. Note that the strange mesons of the opposite C parity are expected to mix.

Thus in a SU(3) symmetric world duality requires the meson SU(3) multiplets to occur in degenerate super multiplets, consisting of octets and singlets of both signatures and with mutually related residues. The observed meson spectrum for both natural and unnatural parity seems to agree reasonably with this super multiplet structure, in the sense that the trajectory split between the four multiplets is no larger than that within a given SU(3) multiplet. Similarly the residues seem to conform to the duality relations.

4.1.3. SU(3) breaking solution. It is appropriate to ask at this point if there is an exact solution to duality, consistent with an appreciable SU(3) breaking in the trajectory functions, as seems to be the case in the real world. The answer is yes and the solution corresponds exactly to the one described in the last section by equations (3.11), (3.12) and (3.9). Assuming Gell-Mann–Okubo mass formula for a broken octet, one can estimate the $I = 0$ mass in terms of the masses of the $I = 1$ and $I = \frac{1}{2}$ members. In particular if the $I = \frac{1}{2}$ mass (eg K*) is appreciably higher than the $I = 1$ mass (eg ρ), then the resulting $I = 0$ mass should be still higher. In this situation duality has a unique solution which requires an SU(3) singlet with a fixed mass and coupling strength and a fixed angle of mixing with the $I = 0$ member of the octet. The required mixing angle is $\tan\theta = (\sqrt{2})^{-1}$, and the singlet mass and coupling are such that, after mixing, one of the $I = 0$ masses overlaps with the $I = 1$ mass and the other $I = 0$ member decouples from channels like $\pi\pi$ and $\pi\rho$. (In addition, of course, pairwise exchange degeneracy between the positive and negative signature trajectories as in equation (3.11) and the corresponding residues must hold.) We have seen in the last section that all the three above conditions are satisfied by the vector and the tensor nonets. The same is not true, however, for the pseudoscalar and axial vector nonets. For instance the mixing angle between η and η', as determined by the Gell-Mann–Okubo mass formula, seems to be roughly equal to zero, and both these masses are substantially higher than the $I = 1$ mass (ie π). It is fair to summarize, therefore, that the duality solution is satisfied more or less exactly for the physical vector and tensor trajectories, whereas for the unnatural parity trajectories they are broken at roughly the same level as SU(3). (See eg Logan and Roy 1971.)

4.2. Meson–baryon scattering

The duality and exoticity constraints in s channel meson–baryon scattering fall broadly into three categories:

(*a*) constraints on meson trajectories (t channel) from exoticity in the meson–baryon (s and u) channels;

(*b*) constraints on baryon trajectories (u channel) from exoticity in the meson–baryon (s) channel;

(*c*) constraints on baryon trajectories (u channel) from exoticity in the annihilation (t) channel.

(*a*) *Meson multiplets from baryon exoticity.* Consider first the pseudoscalar octet–baryon octet scattering PB→PB. The meson super multiplet structure and their couplings to the meson vertex have been completely determined from PP scattering (except for an overall normalization). Thus we have six parameters characterizing their couplings to the baryon vertex—s_T, d_T, f_T for singlet, symmetric

octet and antisymmetric octet couplings of the tensor nonet and similarly s_V, d_V, f_V for the vector nonet. The exoticity in the meson–baryon SU(3) states 10 and 27 (see equation (4.2)) gives two constraints on these six independent couplings. They are (see Mandula *et al* 1970)

$$s_T = d_T \pm 3f_T \tag{4.3}$$

$$d_T - f_T = \pm(d_V - f_V) \tag{4.4}$$

where the sign ambiguity reflects the fact that the meson vertices occur linearly in PB→PB, whereas they are known only in quadratic form from PP→PP. Applying a similar exoticity condition to PB→VB gives relations identical to (4.3) and (4.4) except that the vector and tensor indices are interchanged. Altogether in view of the symmetry of (4.4) one has three constraints amongst the six couplings.

The duality result on the non-pomeron pp total cross section,

$$\sigma_{pp}(\text{non-diffractive}) = 0 \tag{4.5}$$

is often used as a fourth constraint, which is equivalent to

$$f_V/d_V = f_T/d_T. \tag{4.6}$$

The entire vector and tensor nonets are then described by only two independent couplings, which are the d and f. Consequently one has many interesting predictions.

For instance all baryon–baryon cross sections are predicted to be flat, ie

$$\sigma_{BB}(\text{non-diffractive}) = 0 \tag{4.7}$$

and many meson–baryon cross sections are mutually related as shown in table 1.

Table 1. Non-diffractive meson–baryon cross sections

Channel	Relative cross section
K^+p	0
K^+n	0
π^-p	$2f$
π^+p	$f-d$
K^-p	$2f$
K^-n	$f-d$

(*b*) *Baryon multiplets from baryon exoticity.* In this case duality and exoticity constraints do not determine the baryon trajectory spectrum completely. Consider first octet–octet (PB→PB) scattering. There could be *a priori* six degenerate SU(3) multiplets—singlets, octets and decuplets of positive and negative signature. Taking into account the symmetric and antisymmetric octet couplings one has eight independent coupling parameters, $s_\pm$, $d_\pm$, $f_\pm$ and $t_\pm$. There are only two constraints coming from the baryon exoticity in the s channel representation 10 and 27 (see equation (4.2)). In order to complete the picture we also consider meson octet and baryon decuplet scattering

$$8(\times)10 = 8(+)10(+)27(+)35. \tag{4.8}$$

We see from (4.2) and (4.8) that PB→PΔ gives one constraint, corresponding to the exotic channel 27. There are two exotic channels 27 and 35 in PΔ→PΔ. However, the crossing matrix for this process is such that the two degeneracy constraints are the same, so altogether one has four constraints and twelve couplings —$E_\pm$ and $T_\pm$ corresponding to octet and decuplet couplings to the $P\Delta$ channel in addition to the eight couplings above for the PB, as shown in figure 16.

Thus one has a grossly under-determined system. But the constraints give some very interesting results when we supplement them with our experimental knowledge on the baryon spectra. The latter suggests for instance that the giant degeneracy structure involving all the six multiplets is not realized in nature, at least for the prominent trajectories. Therefore, one should look for minimal solutions to the four duality constraints involving a subset of these six.

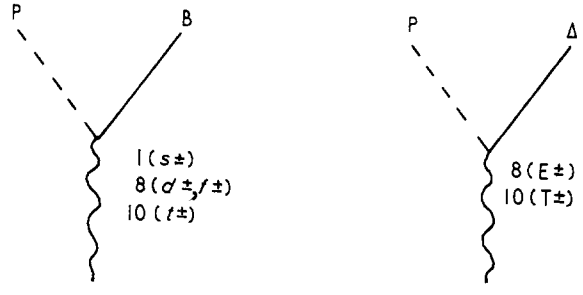

Figure 16. Baryon trajectory coupling to the pseudoscalar and baryon octet (PB) and pseudoscalar and baryon decuplet (PΔ) channels.

Solutions involving four or fewer degenerate trajectories are quoted below from Mandula *et al* (1970):

$$\begin{array}{ll} \text{(i)} \quad 8 \Leftrightarrow 10 & \text{(vi)} \quad 8 \Leftrightarrow 1(+)8(+)10 \\ \text{(ii)} \quad 8 \Leftrightarrow 8 & \text{(vii)} \quad 1(+)8 \Leftrightarrow 8(+)10 \\ \text{(iii)} \quad 8 \Leftrightarrow 8(+)10 & \text{(viii)} \quad 1(+)8 \Leftrightarrow 1(+)8 \\ \text{(iv)} \quad 10 \Leftrightarrow 8(+)10 & \text{(ix)} \quad 8(+)10 \Leftrightarrow 8(+)10 \\ \text{(v)} \quad 8 \Leftrightarrow 8(+)1 & \end{array} \tag{4.9}$$

where the multiplets on the opposite ends of the arrow have opposite signatures. It is easy to see, for instance, that a solution like $10 \Leftrightarrow 10$ is ruled out as it involves only four terms $(t_{\pm}, T_{\pm})$ which get over-determined by the four homogeneous constraints.

The baryon spectrum strongly suggests that there is no other multiplet near the nucleon mass with the same spin–parity $(\frac{1}{2}^+)$ and similarly there is no other $\frac{3}{2}^+$ multiplet near the $\Delta(1238)$. Therefore the nucleon, the leading natural parity baryon, should be associated with solutions (i), (ii), (iii), (v) or (vi), and the leading unnatural parity baryon, $\Delta(1238)$, should be associated with solutions (i) or (iv). The most favoured solution for nucleon is the solution (vi). The $\frac{3}{2}^-$ members of this super multiplet are usually associated with the $N_\gamma(1520)$ octet and a somewhat heavier decuplet $\Delta(1670)$. The favoured solution for $\Delta(1238)$ is solution (i), the positive signature octet being associated with the $\frac{5}{2}^-$ N(1670) resonance. It should be remarked, however, that there is substantial breaking of exchange degeneracy amongst the above trajectories, in particular between the nucleon and $\Delta(1670)$ trajectories, which are separated by roughly one unit.

The relative couplings of the solution (i) to t_-, T_-, d_+, f_+ and E_+ are exactly determined by the four homogeneous constraints. In particular the f/d ratio for the $\frac{5}{2}^-$ octet is predicted to be $-\frac{1}{3}$ which is close to the experimental value of about $-\frac{1}{5}$. The solution (vi) on the other hand involves nine terms, $d_{\pm}$, $f_{\pm}$, $E_{\pm}$, s_-, t_- and T_-, which are left under-determined by the four constraints. Nevertheless,

some interesting relations emerge. For instance, assuming the $\frac{3}{2}^-$ decuplet branching ratio to PB to be small relative to PΔ (ie $t_- \ll T_-$) on the basis of data leads to an f/d ratio of about unity for both the nucleon and the $\frac{3}{2}$ octets. These again are close to the experimental values of 0·6–1 for the nucleon and about 1·2 for $N_\gamma(1520)$.

Finally one should note that the above solutions for the leading natural and unnatural parity baryons form a very simple pattern in terms of SU(6). One has the exchange degeneracy condition between

$$8(\tfrac{1}{2}^+) \Leftrightarrow 1(\tfrac{3}{2}^-)\,(+)\,8(\tfrac{3}{2}^-)\,(+)\,10(\tfrac{3}{2}^-) \tag{4.10}$$

$$10(\tfrac{3}{2}^+) \Leftrightarrow 8(\tfrac{5}{2}^-) \tag{4.11}$$

which is simply an exchange degeneracy between the SU(6) representation 56 (with orbital angular momentum $L = 0$) on the left and the 70 (with $L = 1$) on the right. The degeneracy holds separately for the spin doublet (4.10) and spin quartet (4.11) members of these multiplets.

(*c*) *Baryon multiplets from meson exoticity.* One can get additional degeneracy constraints on the u channel baryon trajectories by considering exoticity in the annihilation (t) channel. Now the annihilation channel $B\bar{B} \to P\bar{P}$ gives two constraints, from the exotic states $(10 + \overline{10})$ and 27; $B\bar{\Delta} \to P\bar{P}$ gives two constraints, from the exotic states $\overline{10}$ and 27 and $\Delta\bar{\Delta} \to P\bar{P}$ gives one constraint, from the exotic state 27. Thus with s and t channel exoticity conditions there are nine duality constraints altogether. These are still not enough to solve for the non-exotic baryon spectrum exactly, since there could in general be six degenerate trajectories with twelve independent couplings. However, they are enough to kill all the physically reasonable subsets of this super multiplet discussed above. In particular they require every decuplet to be accompanied by an octet of the same signature, which does not seem to be the case for $\Delta(\frac{3}{2}^+)$. Anyhow the most reasonable (or rather the least unreasonable) solution for the $\Delta(\frac{3}{2}^+)$ in this case is $10\,(+)\,8 \Leftrightarrow 8\,(+)\,1$, and for the nucleon trajectory it is $8 \Leftrightarrow 8\,(+)\,10$ or $8 \Leftrightarrow 8\,(+)\,1$. The relative residues in each of these two solutions are also determined. For the first solution, for instance, one has either $f_+/d_+ = f_-/d_- = -\frac{1}{3}$ or $f_+ = d_- = 0$, which are in complete disagreement with the experimental values giving $(f/d)_\pm$ about $+1$. In the second solution the f/d ratios are $+1$, but the octets, including the nucleon, decouple from $P\Delta$, which is experimentally unacceptable.

4.3. Baryon–antibaryon scattering

In s-channel $B\bar{B} \to B\bar{B}$ there are two independent exotic states, $(10 + \overline{10})$ and 27. We have seen earlier that the t channel meson trajectories occur in pairs of exchange degenerate nonets. Moreover, their couplings to the $B\bar{B}$ channels are fixed from MM, MB and BB scatterings and from factorization within two independent parameters, namely the magnitude and the f/d ratio of the octet coupling. Thus we have two homogeneous equations to solve for these two coupling parameters which makes it an over-determined system. In other words, for no value of this f/d ratio can both the $(10 + \overline{10})$ and 27 channels be free from resonances. For a reasonable f/d ratio (eg pure f type coupling for the spin non-flip amplitude) one sees that there must be exotic resonances in both $(10 + \overline{10})$ and 27 $B\bar{B}$ channels. Finally these exotic resonances also satisfy the duality constraints for $B\bar{\Delta}$ and $\Delta\bar{\Delta}$ scattering, ie one does not need more resonances in the 35 or 64 multiplets of SU(3) (Rosner 1968).

It should be remarked, however, that duality constraints on the scattering of the above exotic resonances with ordinary mesons and baryons lead to still more exotic resonances—ie those belonging to 35, 64 and still higher multiplets of SU(3). In fact a consistent solution to duality requires a divergent set of more and more exotic resonances for both mesons and baryons (Roy and Suzuki 1969). Such resonances, if present, are of course expected to decouple from the ordinary meson–meson and meson–baryon channels for consistency with our earlier duality solutions, and what is more important, for consistency with data.

4.4. Concluding remarks

In summary, the duality and exoticity conditions for meson–meson scattering provide an exact solution to the degeneracy pattern of exchanged mesons. For meson–baryon scattering these conditions are not sufficient to solve for the exchanged baryon spectrum uniquely, whilst for the baryon–antibaryon scattering the exchanged meson system is over-determined by these constraints. Thus one has either to abandon the duality hypothesis for baryon–antibaryon scattering (ie assume that the t channel Regge terms are built significantly by the non-resonant contributions in the s channel) or else to assume the existence of exotic resonances with significant coupling to the baryon–antibaryon channels. In either case one expects the baryon–antibaryon total cross sections to show significant energy dependence, even for exotic channels. Experimental search for resonance structures in these channels has so far given negative results. It is fair to say, however, that the data are too scanty to rule out the existence of exotic mesons. Moreover such resonances, as one looks for them above the $B\overline{B}$ threshold (> 2 GeV), are expected to be broad. This is because of the many mesonic channels open, although their coupling to each single channel is required to be small. Thus a phenomenological distinction between the resonance and the background contributions—and hence between the two alternatives mentioned above—is likely to be very ambiguous.

4.4.1. Systematics of duality breaking. Assuming the exotic mesons to be absent, at least in the low mass range (< 2 GeV), one sees a nice systematics in the duality breaking. For PP scattering, the exchange degeneracy prediction (between the vector and tensor nonets) agrees with data not only in the particle classification but in their precise trajectory positions as well. For PV and VV scattering, the degeneracy prediction (between the pseudoscalar and axial vector nonets) agrees with the observed particle spectrum but not with their precise trajectory positions. The same is true for meson–baryon scattering, with the exchange degeneracy prediction of equations (4.10) and (4.11). For the baryon–antibaryon channels, however, the predictions do not even agree with the known particle spectrum. For the annihilation channels the degeneracy pattern involves a $\frac{3}{2}^+$ octet trajectory and for $B\overline{B} \to B\overline{B}$ it involves exotic meson trajectories, neither of which has been observed. These trajectories if present, must be very far below the other members of the super multiplet.

The above systematics of duality breaking have been closely analysed by Mandula *et al* (1969b), who have linked it with the increasing thresholds for the above three classes of reactions. Though far from being a rigorous solution to the problem, this reasoning may nonetheless provide a physical insight into the

mechanism of duality breaking. It essentially goes as follows:

(i) Semilocal duality assumes an overlap region between the direct channel resonances and cross-channel Regge terms.

(ii) Saturation by non-exotic resonances in the direct channel is seen to hold experimentally in the low energy range. However, it is very plausible that it may gradually deteriorate as we go to high energies (>2–3 GeV, say) either due to non-resonant contributions from annihilation channels or due to the presence of high mass exotic resonances. Then duality results will be more exact in those cases where Regge behaviour sets in at lower energies.

(iii) Regge behaviour is expected to set in at lower energies for processes with lower thresholds. For instance, for $\pi\pi$ scattering it may set in at about 0·5–1 GeV. But it can set in only by 1·5–2 GeV for $\rho\rho$ or πN scattering and only by 2·5–3 GeV for N$\bar{\text{N}}$ scattering. It is then plausible that the duality results become less and less reliable as we go from PP to VV or PB and then to B$\bar{\text{B}}$ channels.

5. Duality diagrams

All the significant results of factorization, SU(3), exoticity and semilocal duality, described earlier, can be elegantly summarized in a simple diagrammatic representation—the so-called quark duality diagrams. The technique was first suggested by Harari (1969a) and Rosner (1969) and in subsequent years it has played a very useful role, both in the phenomenological applications of duality and also in the context of formal dual amplitudes, to be discussed later.

We shall first describe the rules of constructing and interpreting the duality diagrams and then discuss some of the immediate results that follow from these rules, and finally we shall outline how the rules can be derived starting from factorization, SU(3), exoticity and duality.

5.1. Rules of duality diagrams

5.1.1. Quark contents of hadrons. Each particle is expressed in terms of its quark content. Thus for the s channel scattering $ab \to cd$, each of the four particle lines (see figure 2) would correspond to two quark–antiquark lines for a meson or to three quark lines for a baryon. It is worth listing the quark contents of the important mesons and baryons in terms of the standard quark triplet p, n and λ. They are

$$
\begin{aligned}
\pi^+, \rho^+, A_2^+ &= \mathrm{p}\bar{\mathrm{n}} & \mathrm{p} &= \mathrm{ppn} \\
\pi^-, \rho^-, A_2^- &= \mathrm{n}\bar{\mathrm{p}} & \mathrm{n} &= \mathrm{pnn} \\
\pi^0, \rho^0, A_2^0 &= \frac{\mathrm{p}\bar{\mathrm{p}} - \mathrm{n}\bar{\mathrm{n}}}{\sqrt{2}} & \Lambda &= \mathrm{pn}\lambda \\
& & \Sigma^+ &= \mathrm{pp}\lambda \\
\omega, f &= \frac{\mathrm{p}\bar{\mathrm{p}} + \mathrm{n}\bar{\mathrm{n}}}{\sqrt{2}} & \Sigma^0 &= \mathrm{pn}\lambda \\
\phi, f' &= \lambda\bar{\lambda} & \Sigma^- &= \mathrm{nn}\lambda \\
\mathrm{K}^+, \mathrm{K}^{*+}, \mathrm{K}^{**+} &= \mathrm{p}\bar{\lambda} & \Xi^0 &= \mathrm{p}\lambda\lambda \\
\mathrm{K}^0, \mathrm{K}^{*0}, \mathrm{K}^{**0} &= \mathrm{n}\bar{\lambda} & \Xi^- &= \mathrm{n}\lambda\lambda \\
\mathrm{K}^-, \mathrm{K}^{*-}, \mathrm{K}^{**-} &= \lambda\bar{\mathrm{p}} & & \\
\bar{\mathrm{K}}^0, \bar{\mathrm{K}}^{*0}, \bar{\mathrm{K}}^{**0} &= \lambda\bar{\mathrm{n}} & &
\end{aligned}
\qquad (5.1)
$$

For our purpose the quarks could be purely mathematical objects as we shall be concerned only with their internal quantum numbers, and with none of their dynamical properties. The only dynamical feature assumed above is the ideal mixing for $\omega-\phi$ and $f-f'$, which, however, follows independently from duality.

5.1.2. Planar and nonplanar quark diagrams. Write down all the connected quark diagrams that are possible for $ab\to cd$. For the simplest case of meson–meson scattering connectedness requires that the two $q\bar{q}$ lines of a, must join two of the other three mesons, ie they should not both join on to the quark lines of a single meson. Thus there are three possible diagrams, representing a connected to bc, cd and bd, which are shown in figures 17(a), (b) and (c) respectively. Figure 17(a) is called a planar diagram, while figures 17(b) and (c) are called non-planar diagrams,

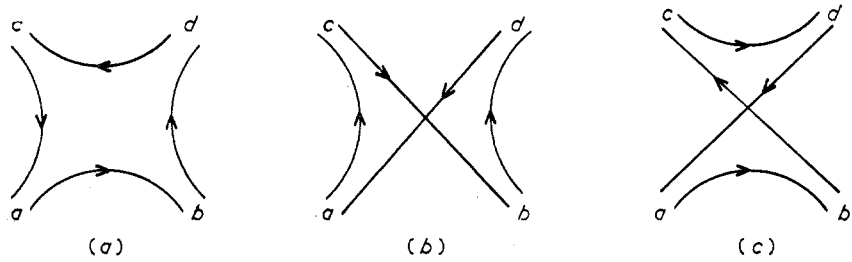

Figure 17. Duality diagrams for meson–meson scattering planar in (a) s-t; (b) t-u; (c) s-u channels.

which reflects the fact that the latter cannot be drawn on a plane without intersecting quark lines. It is clear from this figure that (b) and (c) correspond to planar diagrams between $t-u$ and $s-u$ channels respectively. The connected diagrams for meson–baryon scattering follow an identical pattern, as we see from figures 18(a), (b) and (c). For baryon–antibaryon scattering the only connected diagrams are the ones planar in s-t. There are two such diagrams, shown in figures 19(a) and (b).

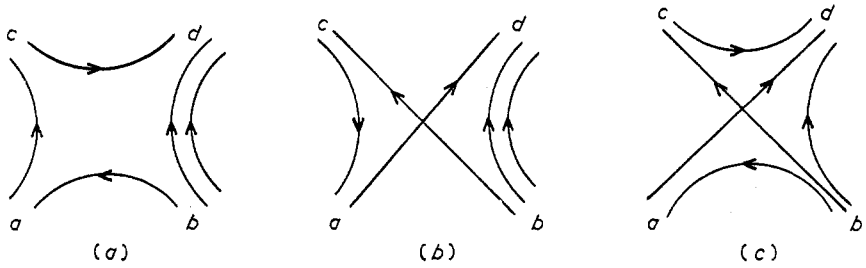

Figure 18. Duality diagrams for meson–baryon scattering planar in (a) s-t; (b) t-u; (c) s-u channels.

5.1.3. Planar diagram and duality. Now the rule can be stated as follows. The scattering amplitude is a sum of all connected diagrams, where each diagram represents a contribution, dual between the two channels in which it has a planar form. Thus for the s channel scattering, $ab\to cd$; the s-t planar diagram (eg figures 17(a), 18(a)) represents a contribution, dual between s channel resonances and t channel Regge poles; and the s-u planar diagram (eg figures 17(c), 18(c)) represents a

contribution, dual between the s channel resonances and u channel Regge poles. In the usual average sense of semilocal duality, therefore, $\mathrm{Im}\,A_s$ is described by the s-t planar diagram alone for large s and fixed t (high energy forward scattering) and by the s-u planar diagram alone for large s and fixed u (high energy backward scattering). The u-t planar diagram (eg figures 17(b), 18(b)) does not contribute to $\mathrm{Im}\,A_s$, but dominates $\mathrm{Im}\,A$ for u channel forward scattering.

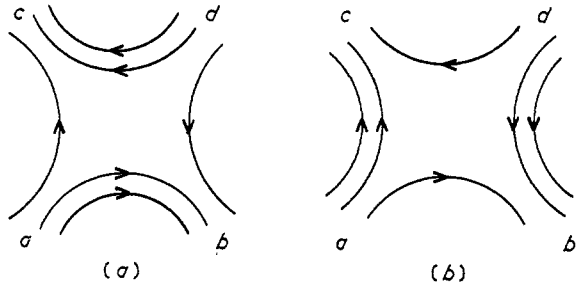

Figure 19. For baryon–antibaryon scattering, the only diagrams possible are those planar in s-t. They correspond to (a) normal resonances in the s channel dual to exotic exchanges in t and (b) exotic resonances in the s channel dual to normal exchanges in t.

One has, of course, no prescription of estimating such diagrams, unlike Feynman graphs. The predictive power of the rule lies in considering such reactions, where some of these types of diagrams cannot be drawn. The average $\mathrm{Im}\,A$ for such cases is then predicted to vanish in an appropriate range of s, t and u.

5.2. Applications

5.2.1. Standard EXD relations. For the s channel reactions $K^+K^+ \to K^+K^+$ and $K^+p \to K^+p$, one easily sees from equation (5.1) that the only connected quark diagrams possible are those of figures 17(b) and 18(b) respectively. The absence of the planar s-t (ie figures 17(a), 18(a)) and s-u (ie figures 17(c), 18(c)) diagrams implies the non-diffractive $\mathrm{Im}\,A_s$ to vanish at high energy, for both forward and backward scattering. These are, of course, the standard results of exchange degeneracy, discussed earlier. It is, in fact, pretty straightforward to derive the general exchange degeneracy result from the duality diagrams. Exotic s channels for meson–meson scattering correspond to 10, $1\bar{0}$ or higher SU(3) representations. These cannot be built from $q\bar{q}$ triplets, as

$$3(\times)\bar{3} = 1(+)8. \tag{5.2}$$

They would require at least four quark ($q\bar{q}q\bar{q}$) lines. Of the three diagrams of figure 17, therefore, only the planar t-u diagram (b) can be present. This implies, in turn, vanishing $\mathrm{Im}\,A_s$ as large s for both fixed t (ie exchange degeneracy in the t channel) and fixed u (ie exchange degeneracy in the u channel). Similarly for exotic meson–baryon channels (ie five quark lines) and all baryon–baryon channels only the planar u-t diagram is present, which gives the standard EXD results.

EXD, SU(3) and factorization also give the equalities

$$\sigma^{\text{Non-Diffractive}}_{\pi^-p(\pi^+p)} = \sigma^{\text{Non-Diffractive}}_{K^-p(K^-n)} \tag{5.3}$$

as we saw in the last section. They follow simply from the duality diagrams; for

example, figure 20. The only difference between the $\pi^- p$ and $K^- p$ case is in the n and Λ quarks, neither of which can, however, annihilate with the baryon quark lines.

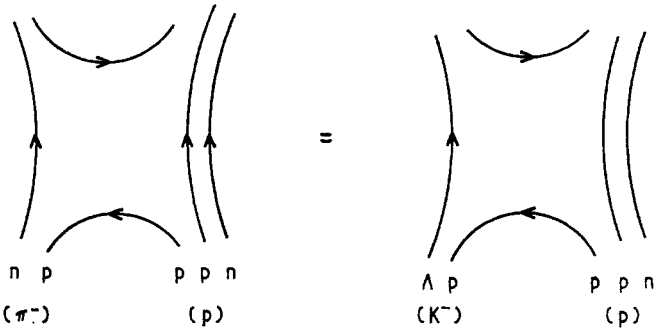

Figure 20. The *s-t* planar diagrams for elastic $\pi^- p$ and $K^- p$ scattering.

5.2.2. Additional EXD relations. Duality diagrams sometimes suggest exchange degeneracy between the *t* channel Regge terms although the *s* channel may not be exotic. The same results, of course, would follow from standard duality and exoticity criteria as well, when one supplements them by factorization and SU(3) considerations. The duality diagrams, however, provide a simple and more transparent method of derivation.

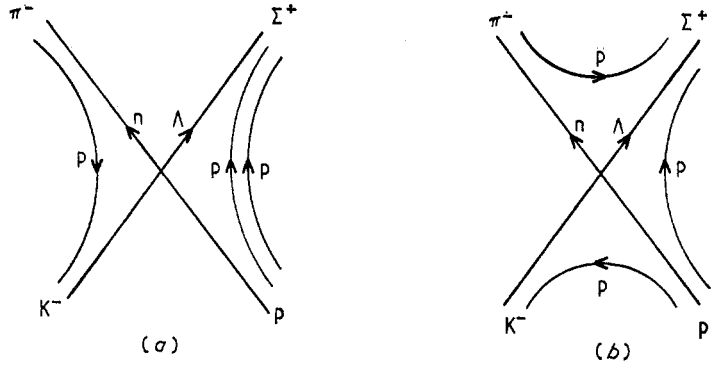

Figure 21. The only diagrams possible for $K^- p \to \pi^- \Sigma^+$ are the ones planar in (*a*) *t-u* and (*b*) *s-u* channels.

The most widely studied examples of this kind are $K^- p \to \pi^- \Sigma^+$ and $K^- n \to \pi^- \Lambda, \pi^- \Sigma^0$. Only two of the three connected diagrams of figure 18 can be drawn for these processes. These are shown in figure 21 for the *s* channel scattering $K^- p \to \pi^- \Sigma^+$. The absence of the *s-t* planar diagram requires $\mathrm{Im}\, A_s$ to vanish for large *s* and fixed *t*—ie the *high energy* resonances should mutually cancel in the forward direction but add up in the backward direction. Alternatively one could apply duality to the exotic channels $K^- \pi^- \to \pi^- K^-$ and $p\Sigma^+ \to \Sigma^+ p$, leading to exchange degeneracy between the K* and K** exchanges in each case. Then factorization would imply exchange degeneracy between these two terms in $K^- p \to \pi^- \Sigma^+$, where the relative sign of the two residues is fixed by that of the ρ-A_2 terms in $K^+ n \to K^0 p$ using SU(3). Thus one gets $\mathrm{Im}\, A_s = 0$.

Experimentally it is not known for certain if exchange degeneracy is broken more strongly for these reactions, compared to the genuine exotic channels like K^+p. But there are some marginal evidences, suggestive of such a breaking.

(*a*) There is substantial breaking of the 'line reversal symmetry' (see equation (2.10)) between the s and u channel reactions $K^-p \to \pi^-\Sigma^+$ and $\pi^+p \to K^+\Sigma^+$. However, this seems to be consistent with $\mathrm{Im}\, A_s = 0$ in some Regge models.

(*b*) There is evidence for significant polarization in the s channel reaction. The polarization test, however, may not be a reliable measure of $\mathrm{Im}\, A_s$, as a relatively small imaginary part (accounting for only 5% of the $d\sigma/dt$, say) may often give rise to a 25% polarization.

(*c*) The resonance contributions to forward $K^-p \to \pi^-\Sigma^+$ have been shown not to cancel mutually, in the sense of semilocal duality; but this has been done only for rather low energy resonances and a very small range of energy.

These questions are receiving substantial experimental and phenomenological attention at present, and one hopes to be able to get a clear picture soon.

5.2.3. Exotic resonances in baryon–antibaryon channels. The exoticity requirement for baryon–antibaryon channels, discussed earlier, can be seen very clearly from the duality diagrams of figure 19. They show that the baryon–antibaryon amplitude consists of two parts—one corresponding to normal ($q\bar{q}$) resonances in the s channel, which is dual to exotic ($q\bar{q}q\bar{q}$) Regge exchanges in t (figure 19(*a*)), and the other corresponding to normal Regge poles in the t channel, which is dual to s channel exotic resonances (figure 19(*b*)). If the high energy non-diffractive cross section is dominated by normal Regge exchanges (as the σ_{pp} data seem to suggest), then it means that the dominant high energy resonances in the $B\bar{B}$ channel must be the exotic ones. In any case it shows that for baryon–antibaryon scattering one should not try to generate the normal t channel Regge poles from the normal s channel resonances in a FESR sense, contrary to some earlier expectations.

5.2.4. Decoupling of ϕ. One easily sees from quark assignment of (5.1) that there is no connected diagram for $\pi^-p \to \phi n$. The same is true for $\pi^+p \to \phi\Delta^{++}$. Thus the high energy cross sections for these reactions are required to vanish, which seems to be supported by data.

5.2.5. Constraint on SU(3) breaking. Duality considerations, supplemented by the observed degeneracy breaking in trajectory functions $\alpha_{\rho,f} > \alpha_{\phi,f'}$, implies a very significant breaking of SU(3) in coupling strengths. For instance the only s-t planar diagrams for s channel π^+p and $K^+\Sigma^+$ scatterings are those of figure 22. Thus the non-diffractive $K^+\Sigma^+$ cross section (involving only ϕ, f' exchange) is predicted to fall rapidly with energy, compared to π^+p (involving only ρ, f exchange). However, the s channel in each case is built out of the same set of resonances—the Δ^{++}s. Thus the branching ratio $\Delta^{++}(M) \to K^+\Sigma^+/\Delta^{++}(M) \to \pi^+p$ is predicted to go down rapidly with the increasing mass of the Δ^{++} multiplets, implying a mass-dependent breaking of SU(3) (Logan and Roy 1970). It is very likely, however, that the physical world corresponds to a significant breaking of duality rather than to a strongly mass-dependent breaking of an internal symmetry scheme like SU(3).

5.2.6. Planarity hypothesis. On a more formal side, the duality diagrams have played a significant role in the context of dual models. In particular figures 17 and 18 suggest that each duality diagram has poles only in the two channels in which

it is planar. For instance figures 17(*b*) and 18(*b*) have no poles in the *s* channel, in which they have exotic quark content of $q\bar{q}q\bar{q}$ and $qqqq\bar{q}$ respectively. Thus for a reaction involving resonant poles in all the three channels the duality diagram rules require the amplitude to be a sum of three parts, each containing poles only in two channels. This assumption is referred to as the planarity hypothesis and it plays a crucial role in the construction of the Veneziano model and its multiparticle generalizations.

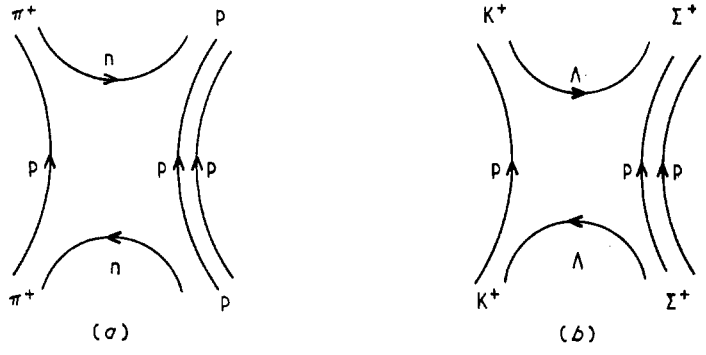

Figure 22. The *s*-*t* planar diagrams for elastic (*a*) $\pi^+ p$ and (*b*) $K^+ \Sigma^+$ scatterings. They correspond to the same set of *s* channel resonances (Δ^{++}) but to different *t* channel exchanges—ρ, f for (*a*) and ϕ, f' for (*b*).

5.3. Derivation

Finally we shall outline how the duality diagram rules can be derived on the basis of duality, SU(3) and factorization (Rosner 1969). We shall restrict ourselves to the simplest example, that of meson–meson scattering. First we write the *s* channel scattering amplitude in terms of the *t* channel Regge poles. It is convenient for this purpose to describe all the four particles as incoming ie the reaction $ab \to \bar{c}\bar{d}$. We then have

$$A_{ab\to\bar{c}\bar{d}} = \sum_e g_{cea}(t)\, g_{d\bar{e}b}(t) \frac{1 \pm \exp(-i\pi\alpha_e)}{\sin \pi\alpha_e} s^{\alpha e} \tag{5.4}$$

where g's are the factorized Regge residues. The summation is over all the vector poles V with negative signature and the tensor poles T with positive signature.

Label the p, n and λ components of the quark triplet by indices 1, 2 and 3 respectively. Now the nonet of vector (and tensor) mesons with ideal mixing, as suggested by duality, constitutes a tensor in the quark space. We have, following (5.1),

$$V_{ij} \equiv (ij) = \begin{vmatrix} \frac{\rho^0 + \omega^0}{\sqrt{2}} & \rho^+ & K^{*+} \\ \rho^- & \frac{\omega^0 - \rho^0}{\sqrt{2}} & K^{*0} \\ K^{*-} & \bar{K}^{*0} & \phi^0 \end{vmatrix} \tag{5.5}$$

and an identical expression for T_{ij}. Here (ij) refer to the two constituent quark vectors. To be consistent with duality we shall assume ideal nonet structure for

any meson multiplet M. Thus the pseudoscalar mesons can be expressed in a tensor form, identical to (5.5). Moreover, following duality, we shall assume the decoupling requirement for the pseudoscalar (eg $\eta' \to \pi A_2$), in addition to those for the vector and tensor mesons.†

Then the SU(3) symmetric couplings for the MMV and MMT nonets are given by

$$\begin{aligned} g_{M_c V M_a} &= \gamma_V \operatorname{Tr}\{V[M_c, M_a]_-\} \\ g_{M_c T M_a} &= \gamma_T \operatorname{Tr}\{T[M_c, M_a]_+\} \end{aligned} \tag{5.6}$$

where the subscripts $-$ and $+$ denote commutator and anticommutator brackets.

The $g_{M_c \bar{V} M_a}$ and $g_{M_c \bar{T} M_a}$ can be obtained from the above expressions too, since $\bar{T}_{ij}$ and $\bar{V}_{ij}$ are simply T_{ji} and V_{ji}.

Writing the above traces in terms of the quark indices,

$$\begin{aligned} g_{M_c V M_a} &= \gamma_V\{(ij)_V (j\bar{k})_c (k\bar{i})_a - (ij)_V (j\bar{k})_a (k\bar{i})_c\} \\ g_{M_c T M_a} &= \gamma_T\{(ij)_T (j\bar{k})_c (k\bar{i})_a + (ij)_T (j\bar{k})_a (k\bar{i})_c\} \end{aligned} \tag{5.7}$$

we see that it consists entirely of connected quark vertices. The disconnected vertices like $\operatorname{Tr}\{V\}\operatorname{Tr}\{M_c M_a\}$ and $\operatorname{Tr}\{T\}\operatorname{Tr}\{M_c M_a\}$ are forbidden by charge conjugation and by the $f' \to \pi\pi$ decoupling requirement respectively. Substituting (5.7) in the amplitude (5.4) then leads to connected quark diagrams only.

Finally we use exchange degeneracy for the residue function

$$\gamma_V = \gamma_T \tag{5.8}$$

and the corresponding relation (3.11) for the trajectories.

Now substituting $g_{M_c V M_a}$, $g_{M_c T M_a}$, $g_{M_d \bar{V} M_b}$ and $g_{M_d \bar{T} M_b}$ from equation (5.7) in (5.4) and using the exchange degeneracy relations we get

$$\begin{aligned} A_{ab\to\bar{c}\bar{d}} = \gamma^2 \frac{s^\alpha ij}{\sin \pi\alpha_{ij}} \{&[(j\bar{k})_c (k\bar{i})_a + (j\bar{k})_a (k\bar{i})_c]\,[(i\bar{l})_d (l\bar{j})_b + (i\bar{l})_b (l\bar{j})_d]\,(1 + \exp(-i\pi\alpha_{ij})) \\ &+ [(j\bar{k})_c (k\bar{i})_a - (j\bar{k})_a (k\bar{i})_c]\,[(i\bar{l})_d (l\bar{j})_b - (i\bar{l})_b (l\bar{j})_d]\,(1 - \exp(-i\pi\alpha_{ij}))\} \end{aligned} \tag{5.9}$$

where $(ij)_e$ has been annihilated with its antiparticle $(ji)_e$. Rearranging the real and complex parts we get

$$\begin{aligned} A_{ab\to\bar{c}\bar{d}} = {} & 2\gamma^2 \frac{s^\alpha ij}{\sin \pi\alpha_{ij}} [(j\bar{k})_c (k\bar{i})_a (i\bar{l})_d (l\bar{j})_b + (j\bar{k})_a (k\bar{i})_c (i\bar{l})_b (l\bar{j})_d] \\ & + 2\gamma^2 \frac{s^\alpha ij}{\sin \pi\alpha_{ij}} \exp(-i\pi\alpha_{ij})\,[(j\bar{k})_c (k\bar{i})_a (i\bar{l})_b (l\bar{j})_d + (j\bar{k})_a (k\bar{i})_c (i\bar{l})_d (l\bar{j})_b]. \end{aligned} \tag{5.10}$$

Following the quark lines of the above expression for A, one immediately sees that the first term corresponds to the nonplanar diagram of figure 17(b), and the second term to the planar diagram of figure 17(a). Thus for high energy forward scattering $\operatorname{Im} A_s$ gets contribution from the planar diagram alone. The nonplanar diagram is purely real here. The real and the complex terms exchange their roles

† The fact that the real pseudoscalar mesons do not conform to ideal nonet structure and to the decoupling requirement assumed here would spoil the coupling relation of (5.6) for vertices involving η or η'. The vertices involving only π's and K's would, however, still obey (5.6).

for negative s (ie u channel) so that $\mathrm{Im}\, A_u$ gets contribution from the nonplanar diagram of figure 17(b). This completes the derivation of the duality diagram rules. Incidentally the third diagram (figure 17(c)) does not contribute to forward (fixed t) scattering for either large s or large u. Hence it does not appear in this derivation. The derivation for meson–baryon or baryon–baryon scattering is in essence similar, but is more complicated algebraically. These are contained in the original paper of Rosner (1969).

5.4. Concluding remarks

In conclusion we wish to stress two points. Since the duality diagram rules can be formally derived from duality, exoticity, SU(3) and factorization, all its predictions can alternatively be obtained, and some of them had first been obtained, from these latter hypotheses. However, these hypotheses, while sufficient to derive duality diagrams, may not all be necessary. Thus it has often been hoped that the duality diagram predictions may be better satisfied in nature than the above set of hypotheses (Harari 1969a).

6. Dual models

6.1. The Veneziano model

To construct an explicit dual model seems a formidable task. For one thing, direct channel resonance terms are polynomials in t, whereas crossed channel Regge pole terms are transcendental functions of t, so we need an infinite number of the former to match the latter exactly. It was therefore a major breakthrough when Veneziano (1968) realized that simple dual model amplitudes could be constructed quite easily.

The Veneziano model was first formulated for the reaction $\pi\pi \to \pi\omega$. Here the s, t and u channels are the same and the T matrix is fully described by a single invariant amplitude $A(s,t,u)$:

$$T = \epsilon_{\lambda\mu\nu\sigma} p_{1\lambda} p_{2\mu} p_{3\nu} e_\sigma A(s,t,u) \tag{6.1}$$

where p_i ($i = 1,2,3$) are the pion momenta and e is the ω polarization vector. Parity conservation allows only ω helicities ± 1 to be produced, so this is an intrinsically spin-flip process; hence the contributions of s channel resonances and t channel Regge poles to A behave like $\mathrm{P}'_J(\cos\theta_s)$ and $\gamma(t)\, s^{\alpha(t)-1}$, respectively.

The ρ Regge pole is the leading singularity in each channel. We therefore want ρ and its recurrences (with $J^{\mathrm{P}} = 1^-, 3^-, 5^-, \ldots$) to appear as low energy resonances; we also wish the high energy behaviour at fixed t to be

$$A \simeq [1 - \exp(-\mathrm{i}\pi\alpha(t))]\, s^{\alpha(t)-1}$$

where $\alpha(t)$ is the ρ trajectory.

After taking part in the construction of some approximately dual amplitudes (Ademollo *et al* 1967, Rubinstein *et al* 1968), Veneziano noticed that the following simple expression has most of the desired properties:

$$A(s,t,u) = \beta\left(\frac{\Gamma(1-\alpha_s)\,\Gamma(1-\alpha_t)}{\Gamma(2-\alpha_s-\alpha_t)} + \frac{\Gamma(1-\alpha_t)\,\Gamma(1-\alpha_u)}{\Gamma(2-\alpha_t-\alpha_u)} + \frac{\Gamma(1-\alpha_u)\,\Gamma(1-\alpha_s)}{\Gamma(2-\alpha_u-\alpha_s)}\right) \tag{6.2}$$

where β is a constant coefficient and α_i denotes the ρ trajectory in the i channel.

This trajectory is assumed linear, ie

$$\alpha_s \equiv \alpha(s) = \alpha_0 + \alpha' s \tag{6.3}$$

and similarly for α_t, α_u. The amplitude (6.2) is clearly analytic and crossing-symmetric; it also has resonance poles and Regge behaviour, and duality between the two, as we see below.

6.1.1. Resonances. The gamma function $\Gamma(x)$ has simple poles at $x = 0$ and at negative integers; the residue at $x = -m$ is $(-)^m/\Gamma(1-x)$. Hence the factors $\Gamma(1-\alpha_s)$ in the first and third terms of equation (6.2) give poles where $\alpha_s = 1, 2, \ldots$. These are more or less the resonance poles that we want. The residue of A at each pole is

$$(\text{Residue at } \alpha_s = N) = \frac{(-)^{N+1}\beta}{\Gamma(N)}\left[\frac{\Gamma(1-\alpha_t)}{\Gamma(2-\alpha_t-N)} + \frac{\Gamma(1-\alpha_u)}{\Gamma(2-\alpha_u-N)}\right]. \tag{6.4}$$

Using the recursion relation $\Gamma(x) = (x-1)\,\Gamma(x-1)$, this reduces to a sum of polynomials in t and u and hence to a polynomial in $\cos\theta_s$, of degree $N-1$. Making a partial wave analysis, into a sum of $P'_J(\cos\theta_s)$ terms, we see that the resonance occurs not just in one partial wave, but in all partial waves with odd $J \leqslant N$. Even J values are forbidden by isospin and Bose statistics for the $\pi\pi$ system; in equation (6.4) this is enforced through the symmetry between t and u.

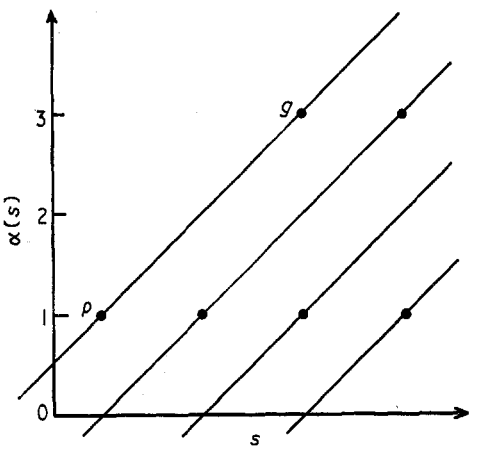

Figure 23. Resonances and trajectories in the $\pi\pi \to \pi\omega$ Veneziano model.

These resonance states are illustrated in figure 23. In addition to the ρ meson and its recurrences on the ρ trajectory, the Veneziano model provides 'daughter' resonances, lying on trajectories spaced at integer intervals below α_ρ; they are required by the model.

The odd daughters (with $J = \alpha$—odd integer) are at first sight particularly surprising, since their masses are not degenerate with the input $\rho, g, \ldots$ etc resonances in this $\pi\pi \to \pi\omega$ case. It was originally proposed to eliminate them by a subsidiary condition

$$\alpha_s + \alpha_t + \alpha_u = 2 \tag{6.5}$$

that is easy to satisfy for strictly linear trajectories. However, we should probably not try to eliminate them. In other contexts (eg $\pi\pi \to \pi\pi$ below) they seem to have

no less physical significance than the even daughters, and there seems to be no prescription for removing them in the general n particle amplitude anyway.

Notice that all resonance poles lie on the real axis of s, and not displaced below it as they should be. This means that the model, as it stands, is not unitary. It gives a zero-width idealization of resonances.

6.1.2. Regge behaviour. Let us see what happens at high energy and fixed t. The Veneziano amplitude (6.2) does not have smooth asymptotic behaviour as $s\to\infty$ along the real axis, because of the successive resonance poles. These poles really ought to lie below the axis. We can therefore correct for this unphysical feature by taking the high energy limit along a ray above the real axis: $s=|s|\,e^{i\phi}$, where ϕ is a small angle and $|s|\to\infty$. The high energy limit defined by this device is smooth. Keeping t fixed the third term in equation (6.2) becomes negligible, and the first two reduce to

$$A(s,t,u)\to\beta\Gamma(1-\alpha_t)\left[(-\alpha_s)^{\alpha_t-1}+(-\alpha_u)^{\alpha_t-1}\right] \tag{6.6}$$

$$\to\frac{\pi\beta}{\Gamma(\alpha_t)}\left(\frac{1-\exp(-i\pi\alpha_t)}{\sin\pi\alpha_t}\right)(\alpha' s)^{\alpha_t-1} \tag{6.7}$$

which is precisely of the required Regge form. In deriving this we have used the relations

$$\Gamma(z+a)/\Gamma(z+b)\to z^{a-b}\qquad\text{as } |z|\to\infty,\qquad 0<\arg z<\pi \tag{6.8}$$

$$\Gamma(x)\,\Gamma(1-x)=\pi/\sin\pi x. \tag{6.9}$$

6.1.3. Duality. This is seen in the fact that the alternative s channel resonance and t channel Regge pictures are constructed from the same terms; they are alternative not additive.

It can be objected that the Regge formulae (6.6)–(6.7) no longer contain s or u channel resonance poles, so that it should be possible in principle to separate resonance and Regge poles into additive terms. Where then is duality? The answer is that such a separation cannot in fact be made if we use only meromorphic functions, which possess poles but no branch points. If we want a duality in which particle poles in crossed channels are dual to each other, and not to various branch cuts instead, the meromorphic assumption is very natural, at least as a first approximation. For fuller discussion, see Oehme (1971).

Some remarks should now be made.

(i) The linearity of trajectories, so that $\alpha_s\to\alpha' s$ as $s\to\infty$, is crucial in getting the Regge pole form above.

(ii) Notice that the Veneziano model automatically gives wrong-signature zeros in the Regge amplitude.

(iii) The coefficient β has to be a constant, independent of s,t,u.

(iv) Within this general framework, we can add 'satellite terms' of the form

$$A'=\beta'\Gamma(K-\alpha_s)\,\Gamma(L-\alpha_t)/\Gamma(M-\alpha_s-\alpha_t)+\text{symmetrical terms}. \tag{6.10}$$

The first term here has resonance poles for $\alpha_s=\text{integer}\ N\geqslant K$; the residue is a polynomial in t of degree $N+L-M$, implying resonance spins $J\leqslant N+L-M+1$. The high energy behaviour is s^{α_t+K-M}. In the present $\pi\pi\to\pi\omega$ example we want leading resonance spins $J=\alpha_s$ and leading Regge behaviour s^{α_t-1}, so we must restrict the satellite terms (6.10) by imposing $M\geqslant L+1$, $M\geqslant K+1$.

(v) The Γ functions in the numerator of a general Veneziano-type term like equation (6.10) give poles at $\alpha_s = \text{integer} \geqslant K$ and $\alpha_t = \text{integer} \geqslant L$. These poles lie on straight lines in the real (s, t) plane, and where they intersect we risk getting double poles. This would be unphysical; the residue of each pole at given s would not be a polynomial in t and hence each pole would represent an infinite set of resonances, with unbounded spins J. Veneziano models avoid double poles through the Γ function in the denominator, which gives lines of zeros at $\alpha_s + \alpha_t = \text{integers} \geqslant M$. These pass through all the intersections of the lines of poles, killing the double poles, provided that $M \leqslant K + L$. This gives one more restriction on the parameters L, K, M.

(vi) The trajectory slopes in different channels should be equal, ie

$$\alpha_s' = \alpha_t' = \alpha_u' = \alpha'.$$

This is trivial in the $\pi\pi \to \pi\omega$ case above since the three channels are identical. In more general cases, however, this is needed so that pairs of contributions such as $(-\alpha_u)^{\alpha_t} \pm (-\alpha_s)^{\alpha_t}$ will reduce asymptotically to a Regge pole term with signature, $(\alpha' s)^{\alpha_t}(1 \pm \exp(-i\pi\alpha_t))$.

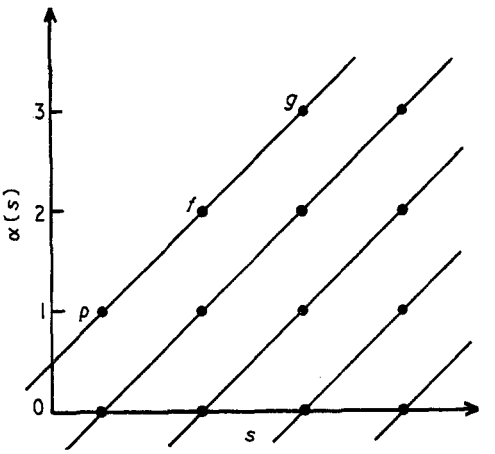

Figure 24. Daughter structure in the $\pi\pi \to \pi\pi$ Veneziano model.

6.2. Various developments

6.2.1. $\pi\pi$ scattering. Having seen how the Veneziano model works in one reaction, we can extend it to others. Consider $\pi^+\pi^- \to \pi^+\pi^-$ scattering (Lovelace 1968, Shapiro 1969). Here the u channel $\pi^+\pi^+ \to \pi^+\pi^+$ is exotic while the s and t channels are identical, so we want a model that involves only s and t channel particles in a symmetrical way. We expect the ρ and f^0 mesons to appear, with their higher spin recurrences and presumably some daughter particles also. We also expect ρ and f^0 (and their daughters too) to be EXD. Since this is a spinless problem, there is only one invariant amplitude A: s channel resonances of spin J contribute $A \simeq P_J(\cos\theta_s)$ and t channel Regge pole exchanges contribute $A \simeq s^{\alpha_t}$. We can meet these requirements by taking

$$A(s,t) = \beta\Gamma(1-\alpha_s)\,\Gamma(1-\alpha_t)/\Gamma(1-\alpha_s-\alpha_t). \tag{6.11}$$

This has sets of resonances at $\alpha_s = N \geqslant 1$ with spins $J \leqslant N$, and is symmetrical between s and t. The pattern of parents and daughters is shown in figure 24.

Bose statistics, coupled with the absence of $I = 2$ exotic states, require us to identify $J =$ odd and even resonances with $I = 1$ and 0, respectively.

The above amplitude $A(s,t)$ is just for $\pi^+\pi^- \to \pi^+\pi^-$ scattering, but through isospin and crossing symmetry it determines all the $\pi\pi$ amplitudes:

$$\begin{aligned} A^0 &= \tfrac{3}{2}A(s,t) + \tfrac{3}{2}A(s,u) - \tfrac{1}{2}A(t,u) \\ A^1 &= A(s,t) - A(s,u) \\ A^2 &= A(t,u) \end{aligned} \tag{6.12}$$

where A^I refers to s channel isospin I.

A nice feature is that this model readily includes the Adler zero, deduced from PCAC consistency (Adler 1965), at the point $s = t = u = m_\pi^2$ when one of the external pions is extrapolated to zero mass. In the Veneziano framework, the only parameter that can change under this extrapolation is the overall factor β, since the trajectories α_i do not depend on external masses; hence we expect this zero to persist. Fortunately, because of the denominator $\Gamma(1-\alpha_s-\alpha_t)$, $A(s,t)$ vanishes on the line $\alpha_s+\alpha_t = 1$. Hence there is a zero at the required place provided $\alpha(m_\pi^2) = \frac{1}{2}$ which is quite compatible with experiment. Satellite terms do not necessarily have this zero, however.

Another nice feature is that essentially all the parent and daughter resonance poles have positive residues. For elastic scattering, a pole residue is essentially the square of a coupling constant. Negative residue poles, sometimes called 'ghosts', are therefore definitely unphysical. Fortunately this π–π model turns out to be ghost-free, with a suitable choice of trajectory (Shapiro 1969).

A less successful aspect is the prediction of daughter particles. There are experimental $J = 0$ candidates that one may identify with the daughter of ρ and grand-daughter of f. Also there is some evidence of a $J = 1$ particle to identify with the grand-daughter of g. But there is no sign whatever of the predicted $J = 1$ daughter of f. (For a recent survey of low energy $\pi\pi$ scattering, see Morgan 1972.) Remember that the prediction of daughter particles is a general feature, not only of Veneziano models, but of any attempt to realize local resonance–Regge pole duality.

6.2.2. The pomeron. The pomeron has not been mentioned above. The Veneziano model is about duality between resonances and Regge poles, ignoring P. If the latter is regarded as a diffractive effect, a consequence of unitarity, we may expect it to appear among the higher order terms of a future complete theory. Meanwhile, any pomeron amplitude has to be added empirically.

6.2.3. Unitarization. The Veneziano model with real trajectories is plainly non-unitary, since all the resonance poles are on the real energy axes. Sometimes this is unimportant; eg in the physical region of K^+p scattering, far from all pole positions, it does not matter that the latter are slightly misplaced. However in other situations, working near a resonance, we must introduce its finite width correctly. Various ways have been tried as discussed below.

(*a*) *Introduce* $\operatorname{Im}\alpha$. Giving α_s a positive imaginary part above threshold ($s > s_0$) displaces resonance poles below the real s axis, but also destroys the linearity of the trajectory below threshold $s < s_0$, since α is an analytic function. This in turn destroys the argument that the pole at $\alpha = N$ represents a set of particles with

spins $J \leqslant N$ and in addition to daughters, we get the undesirable prediction of 'ancestors' with spins $J > N$. There is no evidence for ancestor resonances. A remedy for ancestors is to introduce an imaginary part in α_s only (when working in the s channel physical region), keeping α_t and α_u real and linear as before. This now violates crossing symmetry instead, but has nevertheless sometimes been used as a phenomenological expedient (eg Lovelace 1968).

(*b*) *K matrix prescription.* The K matrix, formally defined by

$$S = 1 + iT = (1 + \tfrac{1}{2}iK)/(1 - \tfrac{1}{2}iK)$$

is a real symmetric matrix. Since the Veneziano formula is also real, it is appealing to identify it with K rather than T. The operator relation $T = K/(1 - \frac{1}{2}iK)$ then automatically converts the real poles of K into complex poles of T. This prescription is only practicable for elastic scattering, possibly including some coupled two-body channels. It then satisfies elastic unitarity but violates crossing symmetry. It has been used, for instance by Lovelace (1969), to calculate $\pi\pi$, πK and $\bar{\text{K}}$K phase shifts.

(*c*) *Smoothing with respect to* α. The poles on the real axis can also be removed by averaging with respect to the parameters of α. For example, we can introduce a parameter λ, such that

$$\alpha_s = \alpha_0 + \alpha' s + \lambda\left(s - \sum_{i=1}^{4} m_i^2\right) \tag{6.13}$$

and similarly for α_t, α_u. We can then replace a given Veneziano amplitude V by

$$\overline{V} = \int_0^{\lambda_0} d\lambda \phi(\lambda)\, V(\lambda) \tag{6.14}$$

where $\phi(\lambda)$ is a weight function vanishing at both limits $\lambda = 0, \lambda_0$.

The result of this averaging is to smear the resonance poles on the real axis into cuts on the real axis, and also to smear Regge poles into Regge cuts. Martin (1969), who suggests this remedy, shows that for suitable weight functions the resonance poles have simply been displaced, and can be reached by analytic continuation through the cuts; also, he shows that Im $\overline{V}$ preserves positivity, ie it has positive Legendre projections in the physical region.

The weakness of this prescription is that it is arbitrary and has no clear physical interpretation.

(*d*) *Dual field theory.* A much more ambitious approach is to regard Veneziano formulae (and their n particle generalizations) simply as analogues of Born approximations in Lagrangian field theory—they are not unitary either. Unitarity is therefore expected to come from adding higher order terms, iterations of Veneziano amplitudes, corresponding to diagrams with closed loops in a field theory. This is an extremely arduous programme, which is by no means complete yet. For a review of progress see Alessandrini *et al* (1971).

6.2.4. Annihilation process $\bar{\text{p}}\text{n} \to \pi^-\pi^-\pi^+$. A very imaginative application was proposed by Lovelace (1968). If $\bar{\text{p}}$n annihilation at rest goes via the S states, as suggested by experiment, the odd-G parity component must come from the $J^{PG} = 0^{--}$ state, with exactly the quantum numbers of a heavy pion. Hence the $\bar{\text{p}}\text{n} \to \pi^-\pi^-\pi^+$ decay amplitude should resemble a $\pi^-\pi^+ \to \pi^-\pi^+$ scattering amplitude (with a

different physical region of course), especially since the Veneziano model has no explicit dependence on external masses.

In fact the $\pi^-\pi^+$ amplitude of equation (6.11) would not fit the $\bar{p}n \to 3\pi$ decay data. The latter have the feature that ρ production is somewhat suppressed; there is an enhancement in the Dalitz plot at the ρ mass, but without the strong angular dependence of a pure ρ signal. Lovelace therefore proposed the alternative form

$$A(s,t) = \frac{\gamma\Gamma(1-\alpha_s)\,\Gamma(1-\alpha_t)}{\Gamma(2-\alpha_s-\alpha_t)}. \tag{6.15}$$

Here s, t, u are the invariant mass-squared for the two $\pi^+\pi^-$ pairs, and $\pi^-\pi^-$, respectively. The numerator Γ-functions give π-π resonance poles in the s and t channels (u is exotic), and the Veneziano formula combines them into a precise dual prescription for overlapping resonance effects. There is no high energy Regge region to concern us here. Formula (6.15) gives resonance poles at $\alpha_s = N \geqslant 1$. The residues are polynomials in t of order $N-1$, so the resonances have spins $J \leqslant N-1$; ie the resonances on the leading trajectory α are all missing—which was the effect desired.

Lovelace noted another interesting property of this formula. The denominator Γ function gives zeros of the amplitude along the straight lines $\alpha_s + \alpha_t =$ integer $N \geqslant 2$. Hence strong suppression is predicted in the Dalitz plot, in all the spaces between the resonance bands, in agreement with experiment. Unfortunately, the full story seems to be more complicated. The ρ resonance is not completely absent, and a detailed fit of the Dalitz plot needs several satellite terms (Altarelli and Rubinstein 1969). Nevertheless, this remains a very pretty illustration.

6.2.5. Baryon poles. An important property of baryon channels is the MacDowell symmetry, which relates partial wave amplitudes with the same angular momentum but opposite parities by

$$f^{J^+}(\sqrt{u}) = -f^{J^-}(-\sqrt{u}) \tag{6.16}$$

where superscripts $\pm$ denote $\tau\mathrm{P} = \pm 1$. Consequently Regge poles occur in opposite parity pairs, with

$$\alpha^+(\sqrt{u}) = \alpha^-(-\sqrt{u}) \tag{6.17}$$

$$\gamma^+(\sqrt{u}) = -\gamma^-(-\sqrt{u}). \tag{6.18}$$

In πN scattering, for example, this symmetry can be seen quite easily. The quantities with simple partial wave decompositions in the u channel are not the invariant amplitudes $A(s,u)$ and $B(s,u)$, but rather the combinations $\tilde{F}^\pm$ (see Barger and Cline 1968):

$$\tilde{F}^\pm(\sqrt{u}, s) = \mp A - (\sqrt{u} \pm M)\,B \tag{6.19}$$

$$\tilde{F}^\pm(\sqrt{u}, s) = \sum_J [f^{J^\pm}\,\mathrm{P}'_{J+\frac{1}{2}}(z) - f^{J^\mp}\,\mathrm{P}'_{J-\frac{1}{2}}(z)] \tag{6.20}$$

where $z = \cos\theta_{\mathrm{cm}}$ in the u channel. Equation (6.19) shows that

$$\tilde{F}^+(\sqrt{u}, s) = -\tilde{F}^-(-\sqrt{u}, s)$$

and the subsequent partial wave decompositions then lead to equation (6.16).

$\tilde{F}^\pm$ are the natural things to Reggeize; each has contributions analogous to equations (2.4) and (2.5). Since $\mathrm{P}'_{J+\frac{1}{2}}$ dominates over $\mathrm{P}'_{J-\frac{1}{2}}$ as $z \to \infty$, for high energy Regge exchange $\tilde{F}^+$ and $\tilde{F}^-$ are dominated by $\tau\mathrm{P} = +1$ and -1 exchanges,

respectively. The natural candidates for Veneziano representations, however, are the invariant amplitudes A and B. These then define the Regge trajectories $\alpha^{\pm}$ appearing in $\tilde{F}^{\pm}$, and the Veneziano coefficients define the residues $\gamma^{\pm}$, through equation (6.19).

An essential part of the Veneziano formula is that trajectories are linear, $\alpha_u = \alpha_0 + \alpha' u$, with no explicit $\sqrt{u}$ dependence. This immediately gives $\alpha^+ = \alpha^- = \alpha_u$, and predicts that particle poles generally occur in degenerate parity doublets, contrary to experiment. This is a serious difficulty. A partial solution is to introduce sums of Veneziano terms and adjust their coefficients so as to cancel some of the unwanted parity partners. The point is that $\sqrt{u}$ dependence enters the residues $\gamma^{\pm}$ through equation (6.19), so by adjusting A and B we can make γ^+ or γ^- vanish at a finite number of $\sqrt{u}$ values (see Inami 1971, Berger and Fox 1971).

An alternative approach is to postulate a fixed cut in the J plane, removing one of the two trajectories $\alpha^{\pm}$ to an unphysical sheet (Carlitz and Kislinger 1970). Then the problem of constructing a dual model still remains (Bardakci and Halpern 1970).

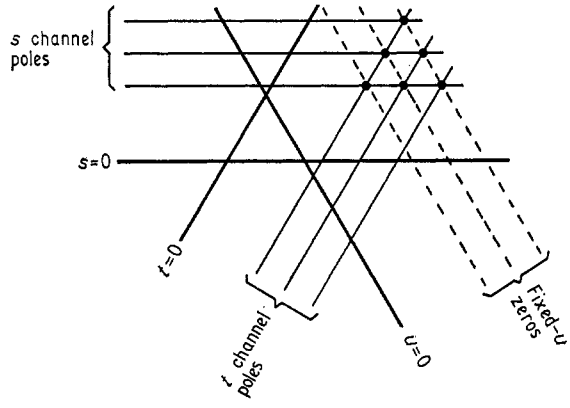

Figure 25. Pattern of poles and zeros in an (s, t) Veneziano term. Solid circles mark pole–pole intersections.

6.2.6. Lines of zeros. In any single Veneziano term

$$V = \frac{\Gamma(K-\alpha_s)\,\Gamma(L-\alpha_t)}{\Gamma(M-\alpha_s-\alpha_t)} \tag{6.21}$$

the denominator Γ function gives zeros on the lines $\alpha_s + \alpha_t = \text{integer} \geqslant M$ that have important physical consequences. In general, the existence of resonance poles at fixed s and fixed t implies that a curve of zeros must pass through each pole–pole intersection to prevent double poles (see discussion in § 6.1). But the Veneziano form implies *in addition* that

(i) these zeros remain on the real s, t plane;
(ii) they lie on straight lines;
(iii) these lines are $\alpha_s + \alpha_t =$ constant (equivalently, $u =$ constant).

These real linear zeros can pass through physical scattering regions and be directly observed. We have already met one example in the $\bar{p}n \to 3\pi$ case above.

Another interesting illustration is $K^- p \to \bar{K}^0 n$, with exotic u channel (Odorico 1971). If it is described by a single Veneziano amplitude like (6.21) we predict dips at fixed u, with a spacing of about 1 $(\text{GeV/c})^2$, appearing in both the s channel and t channel physical regions (see figure 25). In normal Regge theory we might

expect fixed u dips to occur in connection with a u channel exchange; here, on the contrary, u channel exchange is forbidden and the dips come from the interplay of s channel and t channel poles instead. Theoretically, the intersection of the t channel poles ρ, ω, f, A_2 with the s channel poles $\Lambda(1115)$, $\Lambda(1520)$, $\Lambda(1815)$ indicates lines of zeros at $u = 0{\cdot}4$, $-0{\cdot}6$, $-1{\cdot}6$ etc. Experimentally, fixed u dips are found at $u = -0{\cdot}1$, $-0{\cdot}7$, $-1{\cdot}7$. Allowing for some displacement due to Σ resonances, this is a remarkable agreement.

When several different Veneziano terms are added, these zeros do not necessarily survive: unlike poles, zeros are not additive! Nevertheless, Odorico pursued the interesting conjecture that approximately real and linear zeros may be a general feature of scattering amplitudes, ie retaining just property (i) and possibly (ii) above. This idea goes far beyond the simple model from which it started (Odorico 1972).

6.3. Multiparticle amplitudes

6.3.1. Five-particle case. The Veneziano model can be generalized to many-body amplitudes, the simplest case being for five particles. We want a model that will describe intermediate resonance and exchange poles simultaneously, in a dual way.

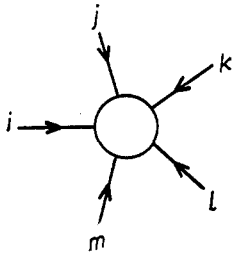

Figure 26. Ingoing particle notation for five-particle amplitudes.

For a symmetrical description, we label all external particles by their *ingoing* momenta p_i and quantum numbers i, with $i = 1, 2, \ldots, 5$ (see figure 26). Thus a typical channel is $1+2 \to \bar{3}+\bar{4}+\bar{5}$, and the same amplitude also describes the nine other channels, $2+3 \to \bar{1}+\bar{4}+\bar{5}$ etc, that are related by crossing. We define

$$s_{ij} = (\mathrm{p}_i + \mathrm{p}_j)^2 \tag{6.22}$$

where s_{ij} is the invariant square of either the ij sub-energy or the ij momentum transfer, depending on the channel.

Figure 27. Single and double pole configurations in five-particle amplitudes.

Single poles are obviously possible in each variable s_{ij}, if the ij quantum numbers are non-exotic (see figure 27(a)). Feynman diagrams show that double poles are also possible, in s_{ij} and s_{lm} simultaneously, provided these are non-overlapping variables, ie the sets $\{ij\}$ and $\{lm\}$ have no common member (see figure 27(b)).

When two channels can have poles separately but not simultaneously, according to Feynman diagrams, we call them 'dual channels'.

The four-particle dual amplitude is generally a sum of (s,t), (t,u) and (u,s) terms. How does this feature generalize? These three terms are associated with the three possible orderings of the particles around the perimeter of a planar duality diagram (see figure 28). (Orderings related by reflection or cyclic permutation are clearly equivalent for this argument.) The ordering *ijkl* corresponds to duality between the *ij* and *jk* channels; this term is absent if either of these channels is exotic or if there is no valid duality diagram. The *ijkl* term is EXD in either the *ij* or *jk* channel; such a term alone gives EXD Regge poles. Two terms corresponding to different orderings must be added, with equal coefficients, to generate a Regge signature factor.

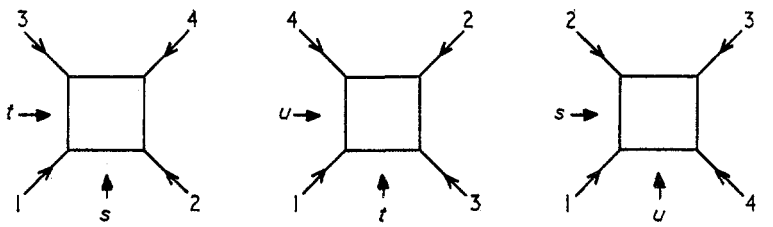

Figure 28. The three independent external orderings in four-particle amplitudes, corresponding to (s,t), (t,u) and (u,s) duality.

Hence we expect the five-particle dual amplitude to be generally a sum of twelve terms, corresponding to the twelve independent orderings of the particles around the perimeter of a duality diagram. The ordering *ijklm* corresponds to duality between the resonance and Regge poles in the channels *ij, jk, kl, lm, mi*, including the admissible double poles, but this term is absent if any of these channels is exotic or if there is no valid duality diagram for this ordering. Any single term will give EXD Regge poles; two different terms with equal coefficients are needed to give a pure signature factor.

Take for example the reaction $K^+p \to K^0\pi^+p$. Out of the twelve independent external orderings, eight are forbidden because the ingoing channels K^+p and $\bar{K}^0\bar{p}$ are exotic. The remaining four are shown in figure 29. Of these, case (d) is forbidden by duality diagram rules; the λ quark line has to connect K^+ to $\bar{K}^0$, and this leads to a non-planar duality diagram unless K^+ and $\bar{K}^0$ are adjacent. Taking diagram (a) alone would give EXD Regge poles, dually related, in the five corresponding channels. Diagram (b) differs from (a) simply by the interchange of π^- and $\bar{p}$: hence if we demand a pure signature factor for the π^+p channel (assuming the single $\Delta(1236)$ trajectory dominates), we must add terms from (a) and (b) with equal strengths and appropriate signs. Similarly we can give the π^-p channel a signature by adding (c) to (b). But such possibilities are very limited; we cannot generate a signature in any other channel using just the allowed diagrams (a), (b) and (c).

What form can each dual term have? An answer is found by studying the integral representation for the Euler B function, occurring in the four-particle case.

$$B_4(\alpha_{12},\alpha_{23}) = \Gamma(1-\alpha_{12})\,\Gamma(1-\alpha_{23})/\Gamma(2-\alpha_{12}-\alpha_{23}) \tag{6.23}$$

$$= \int_0^1 du\, u^{1-\alpha_{12}}(1-u)^{1-\alpha_{23}} \tag{6.24}$$

corresponding to the ordering 1234, where $\alpha_{12} = \alpha(s_{12}) = \alpha_0 + \alpha' s_{12}$ etc. This is completely symmetrical between α_{12} and α_{23}. There are poles in α_{12} at integers $N \geqslant 1$ that can be seen by expanding $(1-u)^{1-\alpha_{23}}$ in a Taylor series and studying the lower limit of u integration. Similarly there are poles in α_{23}, but since the latter are associated with the upper limit of integration, there are no double poles in α_{12} and α_{23} simultaneously.

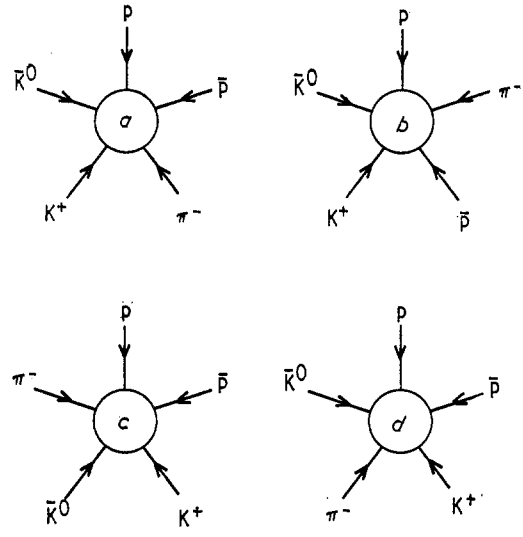

Figure 29. The four non-exotic orderings for the $K^+ p \to K^0 \pi^+ p$ amplitude. Case (d) is forbidden, however, by duality diagram rules.

In direct analogy with equation (6.24), a five-particle generalization corresponding to the ordering 12345 is (Bardakci and Ruegg 1968)

$$B_5(\alpha_{12}, \alpha_{23}, \alpha_{34}, \alpha_{45}, \alpha_{51}) = \int_0^1 \int_0^1 \frac{du_i\, du_j}{1-u_i u_j} u_1^{-1-\alpha_{12}} u_2^{-1-\alpha_{23}} u_3^{-1-\alpha_{34}} u_4^{-1-\alpha_{45}} u_5^{-1-\alpha_{51}} \tag{6.25}$$

where the indices i and j appearing in the integrand are any two *non-successive* integers (modulo 5), and the variables u_k satisfy the constraints

$$u_k = 1 - u_{k-1} u_{k+1}, \qquad (u_6 \equiv u_1). \tag{6.26}$$

Only three of these constraints are linearly independent, leaving two independent variables among the u_k.

This B_5 formula is symmetrical under reflections and cyclic permutations of the ordered variables $\alpha_{12}, \alpha_{23}, \alpha_{34}, \alpha_{45}, \alpha_{51}$. However, it is usual to eliminate some redundant variables, and this symmetry is not then apparent. For example, eliminating u_2, u_3 and u_5 gives the form

$$B_5 = \int_0^1 \int_0^1 du_1\, du_4\, u_1^{-1-\alpha_{12}} u_4^{-1-\alpha_{45}} \left(\frac{1-u_1}{1-u_1 u_4}\right)^{-1-\alpha_{23}} \left(\frac{1-u_4}{1-u_1 u_4}\right)^{-1-\alpha_{34}} (1-u_1 u_4)^{-2-\alpha_{15}}. \tag{6.27}$$

In close analogy with the B_4 case, there are poles at integer values of α_{12} that come from the lower limit of the u_1 integration and can be seen by expanding the integrand

about $u_1 = 0$. Similarly the poles in α_{23} are associated with the neighbourhood of $u_2 = 0$. Double poles cannot occur in the dual channels 12 and 23, because the constraint equation (6.26) prevents u_1 and u_2 from approaching zero simultaneously. However, they are allowed in non-dual channels, such as 12 and 45; this is exactly as we wanted.

It can also be shown that B_5 has other desired properties, such as absence of ancestors and single and double Regge behaviour at high energy. It also has zero-width resonances, and the attendant troubles with unitarity.

Strictly speaking the form of B_5 above is suitable only for scalar external particles, with leading trajectory intercepts $\alpha_0 < 0$. It can be modified by adding an overall kinematic factor to adapt it to the physical trajectories with $\alpha_0 \simeq \frac{1}{2}$, but external fermions still have to be treated as scalars.

The first application was to the reaction $K^- p \to \pi^- \pi^+ \Lambda$ and other reactions, related by crossing and isospin, that share the same amplitude (Petersson and Tornqvist 1969, Tornqvist 1970, Hoyer *et al* 1970). Unfortunately, in this case it was found expedient to use orderings that are forbidden by duality diagram rules. A successful application, respecting these rules, was made to the reactions $K^+ p \to K^0 \pi^+ p$, $K^- p \to \bar{K}^0 \pi^- p$, $\pi^- p \to K^0 K^- p$ that are related by crossing; the allowed diagrams are discussed above and shown in figure 29. It was possible to reproduce all the main features of the data from 2·5–13 GeV/c, including overlapping resonance formation and Regge behaviour, with essentially just one free parameter (Chan *et al* 1970).

Each dual five-particle amplitude describes poles in five channels simultaneously, all tightly interrelated with very few parameters. Even with the freedom of kinematic factors and added satellites these dual amplitudes are much more stringently constrained than their four-particle counterparts. It is remarkable that data fitting is possible at all. For more discussion see the reviews by Berger (1971) and Thomas (1971).

6.3.2. n-particle case. In direct analogy with the previous examples, we expect the n-particle dual amplitude to be a sum of terms corresponding to the $\frac{1}{2}(n-1)!$ independent orderings of the external particles. In any particular case, some may be forbidden by exoticity or by Harari–Rosner rules.

For the kinematics, we now need to define multi-suffixed variables

$$s_{ij\ldots k} = (p_i + p_j + \ldots + p_k)^2. \tag{6.28}$$

Previously these were not needed, because in the five-particle case $s_{123} = s_{45}$. For convenience of notation, let us also consider the case where the external ordering is simply $1, 2, 3, \ldots, n$, and introduce an abbreviation for the variable corresponding to a set of adjacent lines

$$s_{i,k} = s_{i,i+1,i+2,\ldots,k}. \tag{6.29}$$

With the external ordering $1, 2, \ldots, n$, we expect the dual amplitude to have poles in each of the variables $s_{i,j}$ for all possible pairings i, j. These are the energy variables for all the intermediate states, defined by cutting across the duality diagram in all possible ways. If any one of these $s_{i,j}$ channels is exotic the whole term is forbidden.

Multiple poles can also occur, up to order $(n-3)$, in channels that are non-dual, meaning that the corresponding cuts across the duality diagram are compatible. This notion is easier to define using an n-sided polygon, where the sides correspond

to the external particles; then each possible cut (channel) corresponds to a diagonal line joining differing vertices and non-dual channels correspond to non-intersecting diagonals. Note that 'dual' and 'non-dual' are defined with respect to a given ordering. Figure 30 shows an example of three non-dual channels in a six-particle amplitude and a Feynman diagram possessing the corresponding poles.

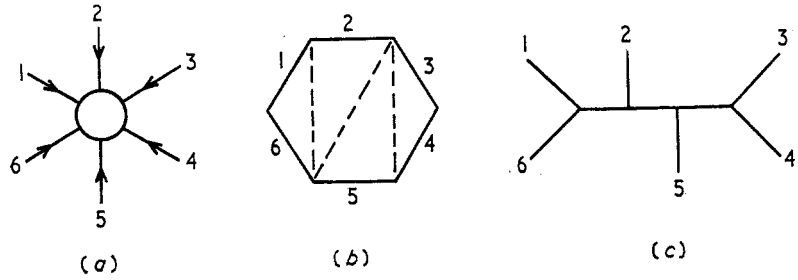

Figure 30. (*a*) An ordered six-particle amplitude; (*b*) non-dual $s_{i,j}$ channels correspond to non-intersecting diagonals of a hexagon; (*c*) Feynman diagram with simultaneous poles in the non-dual channels shown in (*b*).

For brevity we define a label $P = (i,j)$ for each of the contributing channels. We set out to construct an integral representation, in analogy with B_4 and B_5 above, in which the poles in α_P come from the lower limit of integration in an auxiliary variable u_P. To prevent coincident poles in dual channels, we impose constraints

$$u_P = 1 - \prod_{\bar{P}} u_{\bar{P}} \tag{6.30}$$

where the product $\bar{P}$ runs over all channels dual to P. With these constraints it turns out that just $(n-3)$ of the auxiliary variables are independent. An n-particle dual amplitude can then be defined (Chan and Tsou 1969, Goebel and Sakita 1969)

$$B_n = \int_0^1 \prod_P u_P{}^{-1-\alpha_P}\, \mathrm{d}u_P \prod_{P'} \delta\left(u_{P'} - 1 + \prod_{\bar{P}'} u_{\bar{P}'}\right) \tag{6.31}$$

where P runs over all (i,j) channels for the ordering $1, 2, \ldots, n$, and P' runs over all channels excluding a set of $(n-3)$ independent auxiliary variables. This generalized B function is symmetrical under cyclic permutations and reversal of the external particles $1, 2, \ldots, n$, and is analytic apart from poles at values α_P = integer $N \geqslant 0$. Coincident poles in overlapping channels are forbidden by the constraints, built into equation (6.31) through the δ functions. When the δ functions are eliminated, it can be seen that this formula includes our previous B_4 and B_5. For further discussion and references see the reviews by Chan (1970), Alessandrini *et al* (1971) and Veneziano (1970).

7. Duality in inclusive reactions

In the last couple of years there has been immense interest in the study of the so-called inclusive reactions. This has opened a new field for the duality and Regge approach. The simplest duality predictions seem to be borne out by the inclusive data remarkably well. The present section summarizes some of these results.

7.1. Inclusive reactions

Inclusive reactions are processes where one detects and measures only some of the final particles in a collision without caring what else may also be produced. The reaction studied most thoroughly so far is the single particle inclusive reaction

$$ab \to cX \tag{7.1}$$

which represents a sum over all final states containing a given particle c with a given momentum p^c. We have here four invariants—the energy square of $ab(s)$, the momentum transfer squares between $bc(t)$ and $ac(u)$ and the missing mass square (M^2). Only three of these four are independent, since

$$s+t+u = m_a{}^2+m_b{}^2+m_c{}^2+M^2. \tag{7.2}$$

At asymptotic energy the phase space of the final particle c can be divided into two regions. (1) Fragmentation Regions, which correspond to finite t (fragmentation region of (b)) or finite u (fragmentation region of (a)) as s goes to infinity. (2) Central Region, corresponding to both t and u going to infinity along with s.

So far only the fragmentation region has been studied in detail. In view of the essential symmetry between the a and b fragmentation regions, we shall discuss only b fragmentation, ie large s and finite t. In this region the experimental quantities p_{L} and p_{T}, the longitudinal and transverse momentum of c in the rest frame of b, are related to the invariant quantities via

$$\begin{aligned} t &= m_b{}^2+m_c{}^2-2m_b E_c \\ \frac{M^2}{s} &= 1+\frac{p_{\mathrm{L}}}{m_b}-\frac{E_c}{m_b} \\ E_c &= (p_{\mathrm{L}}{}^2+p_{\mathrm{T}}{}^2+m_c{}^2)^{1/2}. \end{aligned} \tag{7.3}$$

Finite t corresponds to finite $p_{\mathrm{L}}, p_{\mathrm{T}}$.

The invariant cross section for (7.1) is

$$s\frac{\mathrm{d}\sigma}{\mathrm{d}t\,\mathrm{d}M^2} = E_c\frac{\mathrm{d}\sigma}{\mathrm{d}p_{\mathrm{L}}\,\mathrm{d}^2p_{\mathrm{T}}} \tag{7.4}$$

which represents the net cross section for $ab \to c(p^c)+$anything. Note that total cross section $\sigma_{ab}^{\mathrm{tot}}$ is formally equivalent to a zero particle inclusive cross section $ab \to$ anything.

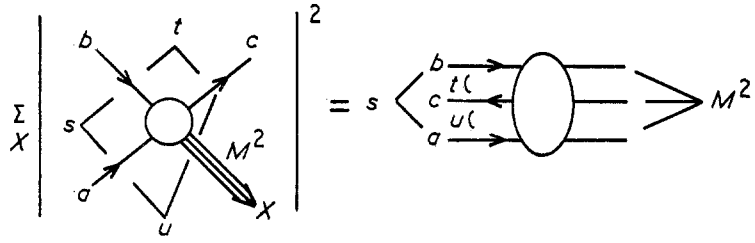

Figure 31. Mueller optical theorem connecting a single particle inclusive cross section to the forward discontinuity of a three-body elastic amplitude.

7.1.1. Mueller's optical theorem. The standard optical theorem (equation (2.6)) connecting the total cross section to the imaginary part of the forward elastic amplitude has been extended to the inclusive cross section by Mueller (1970). This is shown schematically in figure 31. It relates the single particle inclusive

cross section to the forward imaginary part of a three-body elastic amplitude

$$s\frac{\mathrm{d}\sigma}{\mathrm{d}t\,\mathrm{d}M^2} = f = \mathrm{disc}\,A(ab\bar{c}\to ab\bar{c}). \tag{7.5}$$

Of course, the three-body elastic amplitude f is not a physically measurable quantity unlike the two-body case. However, the duality and Regge hypotheses predict many features of this amplitude f, which can be tested with the inclusive cross section data using equation (7.5). This is analogous to testing the exchange degeneracy and Regge behaviour of the two-body elastic amplitude with the total cross section data.

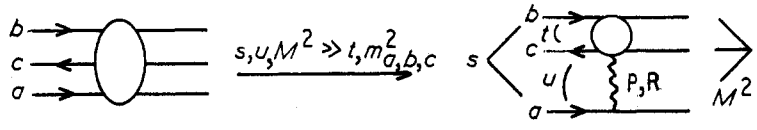

Figure 32. Single Regge expansion of the three-body amplitude for s, u, $M^2 \gg t$, $m_{a,b,c}^2$.

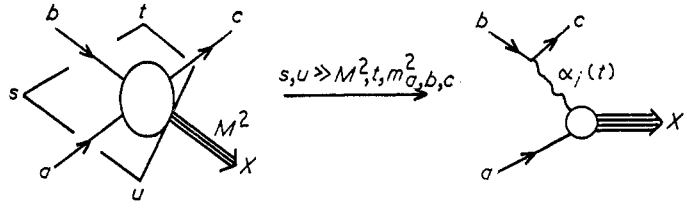

Figure 33. Normal Regge expansion of the amplitude $ab \to cX$ for s, $u \gg M^2$, t, $m_{a,b,c}^2$.

7.1.2. Regge regions. For the Regge analysis of the three-body amplitude f, the fragmentation region (large s, finite t) should be further divided into two parts—large M^2 and large s/M^2. As different quantities become large in these two parts the Regge analyses will be different. The Reggeization condition for a multiparticle amplitude demands that all the invariants spanning across the reggeon be large compared with the ones lying on either end of the reggeon, as we see in figures 32 and 33.

In the Single Regge Region, which has large M^2, the three-body amplitude f can be approximated by the leading Regge exchanges in the $a\bar{a}$ channel, since $s, u, M^2 \gg t$, $m_{a,b,c}^2$ (figure 32), ie

$$f = F_{\mathrm{P}}(t, s/M^2)\, s^{\alpha_{\mathrm{P}}(0)-1} + \sum_{\mathrm{R}=\rho,\omega,f,A_2} F_{\mathrm{R}}(t, s/M^2)\, s^{\alpha_{\mathrm{R}}(0)-1}$$

$$\alpha_P{}^{(0)} = 1, \qquad \alpha_{\mathrm{R}}(0) = \tfrac{1}{2}. \tag{7.6}$$

Here P and R refer to the pomeron and the leading meson trajectories (ρ, ω, f, A_2), which shall be simply called the reggeons. Asymptotically the first term goes to a constant and the second goes down as $s^{-1/2}$. They define the scaling and the non-scaling parts respectively in the terminology of limiting fragmentation (Feynman 1969, Benecke *et al* 1969).

In the Normal Regge Region, with large s/M^2, the production amplitude for (7.1) can be approximated by the leading Regge exchanges in the $b\bar{c}$ channel (figure 33), as $s, u \gg t, M^2, m_{a,b,c}^2$. Hence the cross section is given by figure 34, ie

$$f = s\frac{\mathrm{d}\sigma}{\mathrm{d}t\,\mathrm{d}M^2} = \beta_{ibc}^2(t)\,|\,\xi_i(t)\,|^2\, s^{2\alpha_i(t)-1}\, A_{ia}(M^2, t). \tag{7.7}$$

Here β is the reggeon coupling to $b\bar{c}$, ξ the signature factor and s^{α_i} the reggeon propagator. $A_{ia}(M^2, t)$ is the forward imaginary part of the reggeon particle amplitude.

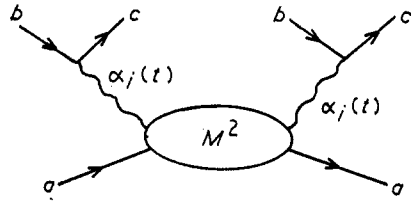

Figure 34. The inclusive cross section for s, $u \gg M^2$, t, $m_{a,b,c}{}^2$.

The Triple Regge Region is defined as having large s/M^2 and large M^2. At sufficiently large s it is possible to have M^2 large, at the same time keeping s/M^2 large. This corresponds to the overlap domain between the two regions described above. In this case figure 34 further reduces to figure 35, which is the so-called

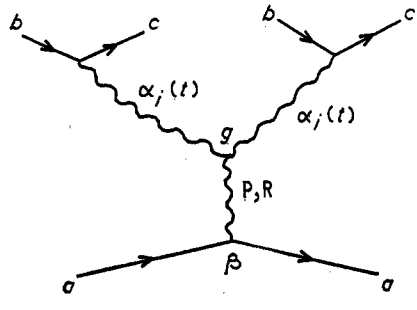

Figure 35. The triple Regge expansion, for large s and large s/M^2.

Triple Regge Graph. It amounts to approximating the reggeon–particle amplitude by the asymptotic contribution

$$A_{ia} \xrightarrow{\text{large } M^2} \beta_{Paa} g^{(t)}_{Pii} (M^2)^{\alpha_P(0)-2\alpha_i(t)} + \beta_{Raa} g^{(t)}_{Rii} (M^2)^{\alpha_R(0)-2\alpha_i(t)}. \tag{7.8}$$

The $2\alpha_i(t)$ term in the exponent arises because the amplitude A_{ia} corresponds to maximal helicity flip of the reggeon legs.

7.1.3. Finite mass sum rule. In a number of models like the perturbation theory and the Veneziano model the reggeon–particle amplitude is seen to have the same analyticity and crossing properties as an ordinary two-particle amplitude (Landshoff 1970, De Tar and Weis 1971). It also has a similar asymptotic Regge behaviour as seen in equation (7.8). It has been postulated, therefore, that the reggeon–particle amplitude satisfies a dispersion sum rule analogous to the FESR (equation 2.13) (Einhorn 1971, Kwiecinski 1972, Olesen 1971, Sanda 1972). This is the finite mass sum rule (FMSR):

$$\int_{\nu_0}^{N} [A_{ia}(\nu, t) - (-)^n A_{\bar{i}a}(\nu, t)] \nu^n \, d\nu$$

$$= \beta_{Paa} g^{(t)}_{Pii} \frac{N^{\alpha_P(0)-2\alpha_i(t)+n+1}}{\alpha_P(0) - 2\alpha_i(t) + n + 1} + \beta_{Raa} g^{(t)}_{Rii} \frac{N^{\alpha_R(0)-2\alpha_i(t)+n+1}}{\alpha_R(0) - 2\alpha_i(t) + n + 1} \tag{7.9}$$

where

$$\nu = \tfrac{1}{2}(M^2 - m_a{}^2 - t). \tag{7.10}$$

By (7.7) the corresponding relation for the inclusive cross section reads

$$\int_{\nu_0}^{N}\left(\frac{\mathrm{d}\sigma}{\mathrm{d}t\,\mathrm{d}\nu} - (-)^n \frac{\mathrm{d}\bar{\sigma}}{\mathrm{d}t\,\mathrm{d}\nu}\right)\nu^n\,\mathrm{d}\nu$$
$$= \beta_{ib\bar{c}}^2(t)\,|\,\xi_i(t)\,|^2\, s^{2\alpha_i(t)-2}\left[\beta_{\mathrm{P}aa}\, g_{\mathrm{P}ii}^{(t)} \frac{N^{\alpha_{\mathrm{P}}(0)-2\alpha_i(t)+n+1}}{\alpha_P(0)-2\alpha_i(t)+n+1}\right.$$
$$\left. + \beta_{\mathrm{R}aa}\, g_{\mathrm{R}ii}^{(t)} \frac{N^{\alpha_{\mathrm{R}}(0)-2\alpha_i(t)+n+1}}{\alpha_{\mathrm{R}}(0)-2\alpha_i(t)+n+1}\right]. \tag{7.11}$$

Note that the missing mass variable M^2 here plays a role analogous to the energy variable in the two-body case.

7.1.4. Dual property of the three-body amplitude. The Harari–Freund two-component duality for the two-body case has been extended to the three-body amplitude (Einhorn *et al* 1971, Tye and Veneziano 1972a,b). In general one gets seven components, with some additional contribution coming from diffraction dissociation if the particles b and c have identical quantum numbers.

In the region of small t, however, the two-component picture is expected to provide a good approximation, ie the resonances and background contributions in $ab\bar{c}$ (or equivalently the missing mass channel X) should be dual to the reggeon and pomeron exchanges in the $a\bar{a}$ channel (Chan *et al* 1971). This can be seen intuitively from figure 29. For small t the system $b\bar{c}$ can be treated as a quasi-particle, moved somewhat off its mass shell. Therefore the three-body amplitude in this limit should not behave very differently from a quasi two-body amplitude. A more formal justification for this ansatz has been provided by Chan and Hoyer (1971) on the basis of dual perturbation theory. The only exceptions to the ansatz are when the $b\bar{c}$ system has exotic or vacuum quantum numbers, the latter containing diffraction dissociation. In either case the identification of $b\bar{c}$ with a quasi-particle system fails.

Experimentally the fragmentation events are heavily concentrated at small p_{T}. As a result a large part of the fragmentation events satisfy the small t criterion, particularly for a light fragment like π. Therefore these events provide a good test for the two-component duality and the Regge theories described above.

7.2. Duality in the large missing-mass region

In high energy two-body scattering the most significant result of duality is the exchange degeneracy. We have seen this firstly in the flatness of the exotic cross sections and secondly in the equality between the non-diffractive components of the total cross sections for $\pi^-\mathrm{p}(\pi^+\mathrm{p})$ and $\mathrm{K}^-\mathrm{p}(\mathrm{K}^+\mathrm{n})$. These two sets of EXD predictions can be extended to the large M^2 inclusive cross section, via two-component duality and the single Regge formula (7.6), as we see below.

(1) Let us compare the set of 'exotic' reactions ($ab\bar{c}$ exotic and $b\bar{c}$ non-exotic)

$$\mathrm{K}^+\mathrm{p}\to\pi^-\mathrm{X}, \quad \pi^+\mathrm{p}\to\pi^-\mathrm{X}, \quad \mathrm{pp}\to\pi^-\mathrm{X}$$

with the 'non-exotic' ones

$$\mathrm{K}^-\mathrm{p}\to\pi^-\mathrm{X}, \quad \pi^-\mathrm{p}\to\pi^-\mathrm{X}, \quad \gamma\mathrm{p}\to\pi^-\mathrm{X}.$$

The six reactions have a common fragmentation vertex ($b\bar{c}$) (compare figure 32).

Assuming pomeron factorization, therefore, the six cross sections should have a common asymptotic limit, when normalized by the corresponding *ap* total cross section ie the ratio $f(ab \to cX)/\sigma(ap)$. Now, the two-component duality predicts the exotic cross sections to have reached this limit already at small s, while the non-exotic ones are predicted to approach this from above following a $s^{-1/2}$ behaviour (see equation (7.6)). The experimental cross sections are, indeed, in good agreement with these predictions as we see in figure 36.

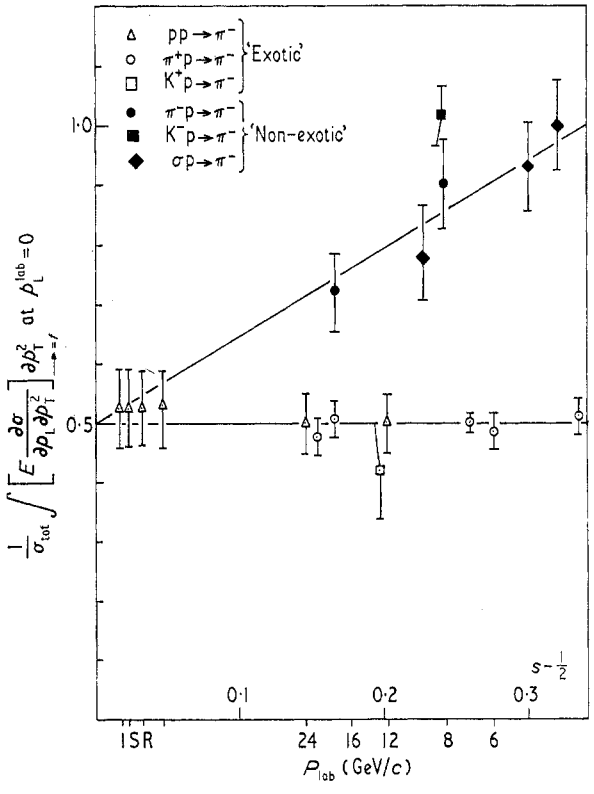

Figure 36. Comparison of the 'exotic' cross sections $(p, \pi^+, K^+)\, p \to \pi^- X$ with the 'non-exotic' ones $(\pi^-, K^-, \gamma)\, p \to \pi^- X$.

There are several technical advantages in testing EXD with the inclusive data compared to the two-body case. Firstly, we see from figure 36 that the non-scaling term here is typically a 50–60% effect, in contrast to the 15–20% effect in the total cross section case. Therefore, the observed flatness of the exotic cross sections here is that much more spectacular a success for duality. Secondly, one has more freedom with the quantum numbers, as one is dealing with a three-body system. Consequently a large number of exotic channels are experimentally accessible here, whereas one had only KN and NN in the total cross section case. We list below the exotic inclusive cross sections where the s independence has been checked, either by comparing data at different energies (where available) or through factorization.

(*a*) $\pi^+ p \to \pi^- X$, (*b*) $K^+ p \to \pi^- X$, (*c*) $pp \to \pi^- X$

(*d*) $K^+ p \to \pi^+ X$ (*e*) $pp \to \pi^+ X$ (*f*) $\pi^+ p \to \Lambda X$

(*g*) $K^+ p \to \Lambda X$, (*h*) $\pi^+ p \to K_s^0 X$, (*i*) $pp \to \Lambda X$.

Finally, in contrast to the total cross section, the s independence of the inclusive cross section can be checked as a function of two extra variables—t and s/M^2 (or equivalently p_L and p_T). Such a two-dimensional test of EXD has, indeed, been made with a large number of inclusive data (Chen *et al* 1971).

(2) Applying EXD, factorization and SU(3) to the single Regge formula (7.6), one gets the additional relations

$$f^{\text{non-scaling}}(K^- p \to \pi^- X) = f^{\text{non-scaling}}(\pi^- p \to \pi^- X) \tag{7.12}$$

and a similar relation between $K^- p \to \pi^- X$ and $\gamma p \to \pi^- X$. These are analogous to the relation (5.3) for the total cross sections. One can check these, for instance, by drawing quark diagrams for (7.12) analogous to figure 20. Again these relations have been found to agree very well with the inclusive data (Miettinen 1972, Chan *et al* 1972).

7.3. Duality in the small missing-mass region

In low energy two-body scattering the most significant result of duality is the Dolen–Horn–Schmid observation that the resonance contributions are interpolated by the leading Reggeon exchange in some average sense. It assumes the FESR (2.14) to hold in a local or semilocal sense in addition to the two-component duality, and we have seen evidence of its success in figures 9–11. The hypothesis can be extended to the inclusive cross section by assuming the FMSR (7.11) to hold semi-locally and, of course, the two-component duality. It gives, for instance,

$$\left\langle \frac{d\sigma^{\text{res}}}{dt} - \frac{d\bar{\sigma}^{\text{res}}}{dt} \right\rangle = \beta_{ibc}^2 |\xi_i(t)|^2 s^{2\alpha_i(t)-2} \beta_{Raa} g_{Rii}(t) \langle \nu_{\text{res}} \rangle^{\alpha_R(0)-2\alpha_i(t)} \tag{7.13}$$

where the averaging is to be taken over resonances in an M^2 interval of about 1 GeV^2, as in the two-body case.

The equation (7.13) is evidently a very powerful relation for the resonance production process (see figure 33):

$$ab \to cj. \tag{7.14}$$

It relates the production cross section to the mass of the produced resonance M_j^2. This relation has been applied to several sets of resonance production data with remarkable success (Hoyer *et al* 1973a, b). We quote a few examples below.

The reactions

$$\pi^- p \to n(\rho^0, f, g^0) \tag{7.15}$$

$$K^- p \to n(K^{*0}, K^{**0}) \tag{7.16}$$

are dominated by pion exchange at small t. Equation (7.13) predicts the production cross section to increase with the resonance mass as

$$\frac{d\sigma_j}{dt} \simeq (M_j^2)^{\frac{1}{2}-2\alpha_\pi(t)}. \tag{7.17}$$

(Note that the crossed reggeon–particle channel $d\bar{\sigma}/dt$ is exotic for the above processes.) The above prediction is compared against the data for (7.15) in figure 37. Similar comparisons have been made for (7.16) and for the f, ω exchange contributions in

$$\pi^- p \to p(\pi^-, \rho^-, A_2^-, g^-) \tag{7.18}$$

$$K^- p \to p(K^-, K^{*-}, K^{**-}). \tag{7.19}$$

In each case one observes rather good agreement.

The relation (7.13) has two significant corollaries.

(1) For a given Regge exchange the production cross section should show a logarithmic antishrinkage with increasing resonance mass.

(2) The ratio of π to f, ω should increase linearly with resonance mass square ($\simeq (M_j^2)^{2\alpha_\pi - 2\alpha_{f,\omega}}$). Again one sees good experimental support for these predictions.

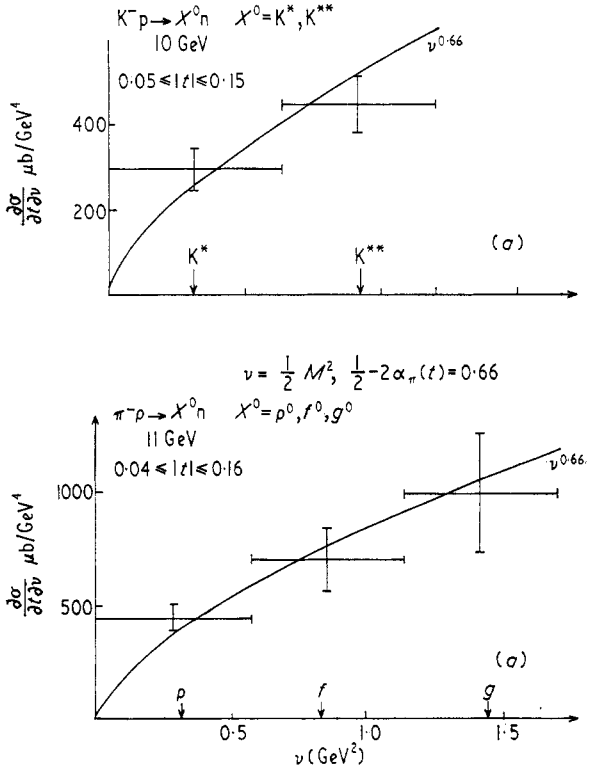

Figure 37. Comparison of the resonance production cross sections

$$\pi^-(\mathrm{K}^-)\,\mathrm{p} \to \mathrm{n}\rho^0, f, g^0(\mathrm{K}^*, \mathrm{K}^{**})$$

with the duality prediction $(M_{\mathrm{res}}^2)^{\frac{1}{2}-2\alpha_\pi(t)}$.

The analysis has been extended to meson–baryon and baryon–antibaryon channels by studying backward resonance production, ie baryon exchange processes. One remarkable result of this analysis is the dual property of meson resonances in the baryon–antibaryon channels. This comes from the backward production process (see figure 33)

$$\mathrm{p}\pi^- \to \mathrm{p}(\pi^-, \rho^-, A_1^-, A_2^-, g^-) \tag{7.20}$$

which is dominated by Δ exchange. One expects that here

$$\frac{\mathrm{d}\sigma_j}{\mathrm{d}t} \simeq (M_j^2)^{\alpha_R(0) - 2\alpha_\Delta(t)}. \tag{7.21}$$

Now, the interpolation of these resonance production cross sections require $\alpha_R(0) \simeq -\frac{1}{2}$, instead of the normal value $+\frac{1}{2}$ observed for the same set of resonances in forward production, ie in the meson–meson channel. This provides the first experimental support for the duality diagram prediction of figure 19 which says that

normal two-quark resonances should be dual to some exotic trajectory exchange in the baryon–antibaryon channel. One should note that such resonances were inaccessible in the two-body case, due to the high threshold of baryon–antibaryon scattering. They could be probed, however, by going into the reggeon–particle channel.

7.4. Concluding remarks

The inclusive reactions provide a much wider scope to study the duality hypothesis compared to the good old two-body phenomenology. The most significant results of duality—ie EXD for high energy scattering and the Regge interpolation of resonances at low energy—have been extended to the inclusive case with remarkable success. However, the inclusive study is still in its preliminary stages. There are continuing developments in this field, on both experimental and theoretical sides. They involve looking into a wider class of fragmentation processes and into other aspects of the subject, such as the central region and the two-particle inclusive reactions etc. These analyses will surely add a great deal to our understanding of duality.

Acknowledgments

We are indebted to our colleagues at the Rutherford Laboratory, especially Chan Hong-Mo, Gordon Ringland, Richard Roberts and Robert Worden, for many valuable discussions and comments.

References

ADEMOLLO M, RUBINSTEIN H R, VENEZIANO G and VIRASORO M A 1967 *Phys. Rev. Lett.* **19** 1402
ADLER S 1965 *Phys. Rev.* **137** B1022
ALESSANDRINI V, AMATI D, LE BELLAC M and OLIVE D 1971 *Phys. Rep.* **1C** 271
ALTARELLI G and RUBINSTEIN H R 1969 *Phys. Rev.* **183** 1469
BARDAKCI K and HALPERN M 1970 *Phys. Rev. Lett.* **24** 428
BARDAKCI K and RUEGG H 1968 *Phys. Lett.* **28***B* 242
BARGER V and CLINE D 1968 *Phenomenological Theories of High Energy Scattering* (New York: W A Benjamin)
BARGER V and MICHAEL C 1969 *Phys. Rev.* **186** 1592
BARGER V and PHILLIPS R J N 1969a *Phys. Rev.* **187** 2210
—— 1969b *Phys. Lett.* **29***B* 676
BENECKE J, CHOU T T, YANG C N and YEN E 1969 *Phys. Rev.* **188** 2159
BERGER E 1971 *Phenomenology in Particle Physics* (Pasadena: California Institute of Technology) p83
BERGER E and FOX G C 1970 *Phys. Rev.* **188** 2120
—— 1971 *Nucl. Phys.* B**26** 1
CAPPS R 1969a *Phys. Rev. Lett.* **22** 215
—— 1969b *Phys. Rev.* **185** 2008
CARLITZ R and KISLINGER M 1970 *Phys. Rev. Lett.* **24** 186
CHAN HONG-MO 1970 *Proc. R. Soc.* A **318** 379
CHAN HONG-MO and HOYER P 1971 *Phys. Lett.* **36***B* 79
CHAN HONG-MO, HSUE C S, QUIGG C and WANG J M 1971 *Phys. Rev. Lett.* **26** 672
CHAN HONG-MO, MIETTINEN H I and LAM W S 1972 *Phys. Lett.* **40***B* 112
CHAN HONG-MO, RAITIO R O, THOMAS G H and TORNQVIST N A 1970 *Nucl. Phys.* B**19** 173
CHAN HONG-MO and TSOU S T 1969 *Phys. Lett.* **28***B* 485
CHEN M S *et al* 1971 *Phys. Rev. Lett.* **26** 1585

CHIU C B and FINKELSTEIN J 1968 *Phys. Lett.* **27***B* 576
CHIU C B and KOTANSKI A 1968a *Nucl. Phys.* B**7** 615
—— 1968b *Nucl. Phys.* B**8** 553
COLLINS P D B, JOHNSON R C and SQUIRES E J 1968 *Phys. Lett.* **27***B* 23
DALITZ R H 1966 *Proc. XIII International Conf. on High Energy Physics* (University of California Press) p215
DE TAR C E and WEIS J H 1971 *Preprint* MIT-CTP 218
DOLEN R, HORN D and SCHMID C 1967 *Phys. Rev. Lett.* **19** 402
—— 1968 *Phys. Rev.* **166** 1768
DONNACHIE A and KIRSOPP R G 1969 *Nucl. Phys.* B**10** 433
EINHORN M B 1971 *Preprint* UCRL-20688
EINHORN M B, GREEN M B and VIRASORO M A 1971 *Phys. Lett.* **37***B* 292
FERRO-LUZZI M, SHEPPARD H K, KERNAN A, POE R T and SHEN B C 1971 *Phys. Lett.* **34** *B*524
FEYNMAN R P 1969 *Phys. Rev. Lett.* **23** 1415
FREUND P G O 1968 *Phys. Rev. Lett.* **20** 235
FUKUGITA M and INAMI T 1972 *Preprint* RPP/T/32
GOEBEL C and SAKITA B 1969 *Phys. Rev. Lett.* **22** 259
HARARI H 1968 *Phys. Rev. Lett.* **20** 1395
—— 1969a *Phys. Rev. Lett.* **22** 562
—— 1969b *Brookhaven Summer School Lectures: BNL Report* (unpublished)
—— 1971 *Phys. Rev. Lett.* **26** 1400
HARARI H and ZARMI Y 1969 *Phys. Rev.* **187** 2230
HOYER P, PETERSSON B and TORNQVIST N A 1970 *Nucl. Phys.* B**22** 497
HOYER P, ROBERTS R G and ROY D P 1973a *Nucl. Phys.* B**56** 173
—— 1973b *Phys. Lett.* **44***B* 258
INAMI T 1971 *Prog. Theor. Phys.* **45** 1903
JACOB M 1969 *Acta Physica Austriaca* Supplementum VI
JACOB M and CHEW G F 1964 *Strong Interaction Physics* (New York: W A Benjamin)
KERNAN A and SHEPPARD H K 1969 *Phys. Rev. Lett.* **23** 1314
KUGLER M 1970 *Acta Physica Austriaca* Supplementum VII
KWIECINSKI J 1972 *Nuovo Cim. Lett.* **3** 619
LANDSHOFF P V 1970 *Nucl. Phys.* B**15** 284
LOGAN R K and ROY D P 1970 *Nuovo Cim. Lett.* **3** 517
—— 1971 *Nuovo Cim.* **3**A 241
LOVELACE C 1968 *Phys. Lett.* **28***B* 264
—— 1969 *Proc. Argonne Conference on $\pi\pi$ and $K\pi$ Interactions; ANL Report* (unpublished)
MANDELSTAM S 1968 *Phys. Rev.* **166** 1539
MANDULA J, REBBI C, SLANSKY R, WEYERS J and ZWEIG G 1969a *Phys. Rev. Lett.* **22** 1147
MANDULA J, WEYERS J and ZWEIG G 1969b *Phys. Rev. Lett.* **23** 266
—— 1970 *Ann. Rev. Nucl. Sci.* **20** 289
MARTIN A 1969 *Phys. Lett.* **29***B* 431
MIETTINEN H I 1972 *Phys. Lett.* **38***B* 431
MORGAN D 1972 *Proc. Seventh Finnish Summer School in Physics, Loma-Koli, Finland* ed Re Pellinen; *Rutherford Report* RPP/T/27
MUELLER A H 1970 *Phys. Rev.* D**2** 2963
ODORICO R 1971 *Phys. Lett.* **34***B* 65
—— 1972 *Nucl. Phys.* B**37** 509
OEHME R 1971 *Springer Tracts in Modern Physics* Vol 57 p119
OLESEN P 1971 *Preprint* CERN-TH-1376
OMNÈS R and FROISSART M 1963 *Mandelstam Theory and Regge Poles* (New York: W A Benjamin)
PETERSSON B and TORNQVIST N A 1969 *Nucl. Phys.* B**13** 629
PHILLIPS R J N and RINGLAND G A 1972 *High Energy Physics* Vol V (New York and London: Academic Press) p187
ROSNER J L 1968 *Phys. Rev. Lett.* **21** 950
—— 1969 *Phys. Rev. Lett.* **22** 689
ROY D P 1971 *Nuovo Cim. Lett.* **2** 545

ROY D P and SUZUKI M 1969 *Phys. Lett.* **28***B* 558
RUBINSTEIN H R, SCHWIMMER A, VENEZIANO G and VIRASORO M A 1968 *Phys. Rev. Lett.* **21** 491
SANDA A 1972 *Phys. Rev.* D**6** 280
SCHMID C 1968 *Phys. Rev. Lett.* **20** 628
—— 1969 *Nuovo Cim. Lett.* **1** 165
SCHWARZ J H 1967 *Phys. Rev.* **159** 1269
SHAPIRO J 1969 *Phys. Rev.* **179** 1345
SINGH V 1963 *Phys. Rev.* **129** 1889
THOMAS G 1971 *Proc. Colloquim on Multiparticle Dynamics* (Helsinki: Research Institute for Theoretical Physics) p418
TORNQVIST N A 1970 *Nucl. Phys.* B**18** 530
TYE S H and VENEZIANO G 1972a *Phys. Lett.* **38***B* 30
—— 1972b *CERN Preprint* TH-1552
VENEZIANO G 1968 *Nuovo Cim.* **57***A* 190
—— 1970 *Lectures at 1970 Erice Summer School*